

Privacy, Interpretability, and Fairness in the Multilingual Space

Anonymous ACL submission

Abstract

Multilingual generalization or compression is an objective for cross-lingual models in natural language processing (NLP). We explore how the compression sought for in such models aligns with other common objectives in NLP such as performance, differential privacy, interpretability, and fairness. We show that compression, which can be quantified by, e.g., sentence retrieval or centered kernel alignment, is compatible with performance and privacy, but that performance and privacy are at odds, leading to non-linear interactions between compression, performance, and privacy. We also demonstrate that privacy is at odds with interpretability, leading to non-linear interactions between compression, privacy, and interpretability. Finally, while fairness and privacy are generally at odds, we show that in the multilingual space, fairness and privacy have common solutions. In sum, our study shows that if we want to learn multilingual models that exhibit good performance and good generalization properties, *and* are private, interpretable and fair (or any combination thereof), we need to jointly optimize for these inter-dependent objectives.¹

1 Introduction

Multilingual NLP models facilitate transfer between closely related languages, but less so across typological divides, language families, or scripts (Singh et al., 2019). Cross-lingual generalization is the objective of multilingual models and a result of *multilingual compression* (Dufter and Schütze, 2020; Ravishankar and Søgaard, 2021), i.e., semantically equivalent expressions being encoded in the same way across languages. If multilingual models compartmentalize languages with different scripts, for example, compression is suboptimal.

NLP for low-resource and medium-resource languages today relies heavily on multilingual models. Language models (LMs) such as mBERT (Devlin

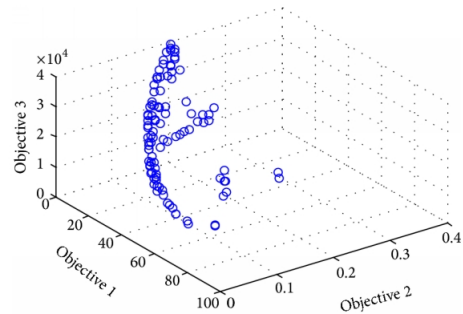


Figure 1: Non-linear interactions in multilingual learning with multiple objectives, e.g., minimizing Objective 1 may lead to high values w.r.t. Objective 3. If we want to optimize for all Objectives 1-3 in such a landscape, we need to do so *jointly*.

et al., 2019) and XLM-RoBERTa (XLM-R; Conneau et al., 2020a) are used as pretrained models for a wide range of real-world applications in many languages—e.g., from named entity recognition (Khalifa et al., 2021) to legal document classification (Wang and Banko, 2021).

With the widespread adaptation of multilingual models comes responsibility. For NLP models to be trustworthy (Pruksachatkun et al., 2021), they must satisfy other requirements, including privacy, interpretability, and fairness. Privacy here means that individual data points cannot be derived from the final model (Dwork et al., 2006). Interpretability means that the training data points that had influence on a prediction can be identified (Koh and Liang, 2017). Fairness refers to equal performance across groups (Hansen and Søgaard, 2021).

Privacy, interpretability, and fairness have primarily been considered in a monolingual context, and it has been assumed that they are largely independent of another, enabling us to develop techniques for one at a time. Our paper presents a *preliminary exploration of the extent to which these objectives align or are at odds*. We explore this in a multilingual context and show how multilingual-

¹Our code and models are publicly available at [URL].

ity presents options and challenges.² Our results indicate that privacy, interpretability, and fairness interact in non-linear ways. Such non-linear interactions mean we have to optimize for all dimensions jointly; see Figure 1 for an illustration.

Contributions In §2, we begin with a theoretical exploration of differential privacy, interpretability, and fairness in the context of multilingual NLP. We show that differential privacy and interpretability are fundamentally at odds,³ a result which is not limited to the multilingual setting. We also show that differential privacy and fairness, often said to be at odds, are compatible in the multilingual setting, as a result of compression. Subsequently (in §3–§5), we present empirical results on the impact of differentially private fine-tuning on multilingual compression and interpretability: We analyze the effect of such fine-tuning on the multilingual compression of large LMs and find that it is possible to achieve (i) high compression with strong privacy at the cost of performance; (ii) high compression with high performance at the cost of privacy; or (iii) privacy and accuracy at the cost of compression. Since we show in §2 that performance, privacy and compression *are theoretically* compatible, this leaves us with an open problem: How do we practically optimize for both performance, privacy and compression? We compare four metrics for quantifying multilingual compression—sentence retrieval, centered-kernel alignment (CKA; Kornblith et al., 2019), IsoScore (Rudman et al., 2021), representational similarity analysis (RSA; Kriegeskorte et al., 2008; Edelman, 1998)—and discuss their usefulness for balancing these trade-offs. Finally, we show that LMs exhibiting high multilingual compression are less interpretable in the sense that they prohibit identifying and tracing back influential examples. In sum, our work shows that *fair and private high-performance multilingual models are possible, even if learning them is challenging. Such models will not be interpretable, however.*

2 Theoretical Exploration

This paper considers language model learning and fine-tuning in a multilingual setting, in which our

²We are, to the best of our knowledge, also first to consider differential privacy in a multilingual setting.

³Naidu et al. (2021) show that differential privacy and GradCAM (Selvaraju et al., 2019), a feature attribution method, are compatible, but no one has, to the best of our knowledge, considered the interaction of differential privacy and instance-based interpretability.

training data $D = D_1 \cup \dots \cup D_{|L|}$ is the union of disjoint training data from $|L|$ different languages. We consider the interaction of differential privacy, interpretability and fairness, with performance and compression in this setting.

Preliminaries We briefly introduce our formal definitions here: A model \mathcal{M}_D induced from a dataset D is said to be ϵ_p -*differentially private* (Dwork, 2006) iff for all datasets D, D' s.t. $D = D' \cup \{x_{diff}\}$, it holds that $\Pr[\mathcal{M}_D(x_{test}) = y] \leq \exp(\epsilon_p) \cdot \Pr[\mathcal{M}_{D'}(x_{test}) = y]$ for any x_{test} and y .⁴ A model \mathcal{M}_D is said to be *interpretable* iff for an unseen data point, x_{test} , it holds that the most influential training data point under leave-one-out influence, x_{diff} , s.t. $D = D' \cup \{x_{diff}\}$ and $D' = \arg \max_{D''} \Pr[\mathcal{M}_D(x_{test})] - \Pr[\mathcal{M}_{D''}(x_{test})]$,⁵ had more influence on \mathcal{M}_D than any other data point $x' \in D$ with $x_{diff} \neq x'$, by some margin ϵ_i , i.e., $(\Pr[\mathcal{M}_D(x_{test})] - \Pr[\mathcal{M}_{D'}(x_{test})]) > \exp(\epsilon_i) \cdot (\Pr[\mathcal{M}_D(x_{test})] - \Pr[\mathcal{M}_{D''}(x_{test})])$ for $D = D'' \cup \{x'\}$. Finally, a model \mathcal{M} is said to be fair if for a group partitioning $g(D) \rightarrow D_{g_1}, \dots, D_{g_n}$ into smaller samples and for some loss function ℓ , e.g., 0-1 loss, $\ell(\mathcal{M}(D_{g_i})) = \ell(\mathcal{M}(D_{g_j}))$. In the following paragraphs, we discuss under what conditions differential privacy, interpretability, and fairness are at odds, and under what conditions they are compatible, and how these conditions align with common scenarios in multilingual NLP.

Differential Privacy and Interpretability We first derive the result that differential privacy and interpretability, as defined in the above, are fundamentally at odds. This result is not limited to the multilingual setting. To see this, recall a model \mathcal{M}_D is differentially private when $\Pr[\mathcal{M}_D(x_{test}) = y] \leq \exp(\epsilon_p) \cdot \Pr[\mathcal{M}_{D'}(x_{test}) = y]$. \mathcal{M}_D is said to be interpretable if $(\Pr[\mathcal{M}_D(x_{test})] - \Pr[\mathcal{M}_{D'}(x_{test})]) > \exp(\epsilon_i) \cdot (\Pr[\mathcal{M}_D(x_{test})] - \Pr[\mathcal{M}_{D''}(x_{test})])$ for $D = D'' \cup \{x'\}$. Assume \mathcal{M}_D is interpretable. We show that the interpretability of \mathcal{M}_D implies that \mathcal{M}_D is not differentially private. This follows from the fact that since \mathcal{M}_D is interpretable, by definition of interpretability, there is at least one data

⁴Note how standard empirical risk minimization is not private, since it is a linear combination of training samples near the decision boundary, and if D and D' differ in one of those, the classifier changes significantly.

⁵It is not feasible to compute leave-one-out influence in practice, but we rely on a commonly used approximation (Pruthi et al., 2020).

point x_{diff} that is revealed by a margin ε_i when applying \mathcal{M}_D to unseen data points. For any ε_i , there is thus a corresponding value ε_p such that \mathcal{M}_D is *not* ε_p -differentially private.⁶ Since the relation between ε_i and ε_p is monotonic, there is no optimal trade-off between the two.

Differential Privacy and Fairness Fairness and privacy are occasionally at odds, as shown in Bagdasaryan et al. (2019); Agarwal (2021),⁷ but in the multilingual setting, fairness and privacy can be compatible. We first note that there is a trivial solution to obtaining differential privacy and fairness (a joint optimum), namely randomness. Next, imagine a perfectly compressed multilingual model \mathcal{M}_D trained on parallel data from $|L|$ languages, $D = \{\dots, i_1, \dots, i_{|L|}, \dots\}$ with i_j and i_k being translation equivalents. Since \mathcal{M}_D is perfectly compressed, at any layer l , the representation of i_j is identical to i_k , i.e., $\mathcal{M}_D^l(i_j) = \mathcal{M}_D^l(i_k)$. This means, by definition, that \mathcal{M}_D is ε -differentially private (for any ε). If fairness is defined in terms of groups that correspond to the set of languages L , as in Choudhury and Deshpande (2021); Anonymous (2022b); Wang et al. (2021), \mathcal{M}_D is also fair. For any other group partitioning, this is not necessarily true, but it should be easy to see that nothing prevents \mathcal{M}_D from being fair, just because it is private. In fact, if \mathcal{M}_D is fair in just one of the source languages $s \in L$, it is globally fair.

3 Experimental Setup

In our experiments, we probe the relation between the performance and compression of fine-tuned multilingual language models, and their privacy and interpretability. We rely on a commonly used multilingual pretrained language model, which we fine-tune with different levels of (ε, δ) -differential privacy on two tasks and probe using metrics of compression and interpretability.⁸ This section presents the pretrained language model, the tasks, the training protocol, the metrics of compression and interpretability, and the evaluation procedure.

Model We use a pretrained XLM-R Base (Conneau et al., 2020a), which has ~ 277 M parameters.

⁶This result generalizes to (ε, δ) -differential privacy if we assume \mathcal{M}_D is influenced by more than δ training points.

⁷Several authors have considered practical trade-offs, including Jagielski et al. (2019), Lyu et al. (2020), Pannekoek and Spigler (2021), and Liu et al. (2021a).

⁸For completeness, we explain the difference between ε -DP and (ε, δ) -DP in Appendix B.

Language	ISO	Family	Script	Tokens (M)	Size (GiB)
Arabic	AR	Afro-Asiatic	Arabic	2869	28.0
Bulgarian	BG	Indo-European	Cyrillic	5487	57.5
Chinese	ZH	Sino-Tibetan	Chinese	435	63.5
French	FR	Indo-European	Latin	9780	56.8
German	DE	Indo-European	Latin	10297	66.6
Greek	EL	Indo-European	Greek	4285	46.9
Hindi	HI	Indo-European	Devanagari	1803*	20.7*
Indonesian	ID	Austronesian	Latin	22704	148.3
Italian	IT	Indo-European	Latin	4983	30.2
Japanese	JA	Japonic	Japanese	530	69.3
Kiswahili	SW	Niger-Congo	Latin	275	1.6
Korean	KO	Koreanic	Korean	5644	54.2
Portuguese	PT	Indo-European	Latin	8405	49.1
Russian	RU	Indo-European	Cyrillic	23408	278.0
Thai	TH	Kra-Dai	Thai	1834	71.7
Turkish	TR	Turkic	Latin	2736	20.9
Urdu	UR	Indo-European	Arabic	815*	6.2*
Vietnamese	VI	Austro-Asiatic	Latin	24757	137.3

Table 1: Overview of languages used in our experiments. Tokens (in millions) and size (in Gibibytes) refer to the respective monolingual corpora in XLM-R’s pretraining corpus. Numbers taken from Conneau et al. (2020a). * includes romanized variants also used in pretraining.

Tasks and Data We fine-tune in a zero-shot cross-lingual transfer setting for POS tagging and NLI. Why these tasks? First, while POS tagging is driven by lower-level syntactic features, NLI requires a higher-level understanding (Lauscher et al., 2020). Second, we can leverage *multi-parallel* corpora for multilingual fine-tuning and zero-shot cross-lingual transfer in both tasks, thereby eliminating potential confounding factors.⁹

For POS tagging, we use the Parallel Universal Dependencies (PUD) treebank from Universal Dependencies (UD) v2.8 (Nivre et al., 2020; Zeman et al., 2021), which contains 1000 sentences parallel across 15 languages. We train in 7 of these languages (FR, IT, JA, PT, TH, TR, ZH), exclude English,¹⁰ and use the remaining 7 languages (AR, DE, ES, HI, ID, KO, RU) for validation. This split ensures that (1) we both train and evaluate on typologically diverse language samples, (2) there exist additional UD v2.8 treebanks in our validation set languages that we can harness for testing, and (3) there exist parallel sentences in our training set languages that we can harness to evaluate multilingual compression. We use the test splits of the following treebanks for testing: Arabic-PADT, German-GSD, Spanish-GSD, Hindi-HDTB, Indonesian-GSD, Korean-Kaist, and

⁹One limitation of this selection is that we only consider classification but no generative tasks, which could be worth exploring in the future.

¹⁰We exclude English to keep the number of languages balanced and because the combined corpus is already biased towards Indo-European with Latin scripts (see Table 1).

Russian-SynTagRus. Appendix Table 3 lists the treebanks’ sizes.¹¹

For NLI, we rely on the XNLI dataset (Conneau et al., 2018), which contains premise–hypothesis–label triples multi-parallel across 15 languages. We, again, train in 7 of these languages (BG, ES, FR, HI, TR, VI, ZH), exclude the original English data, and validate in the remaining 7 languages (AR, DE, EL, RU, SW, TH, UR). We train and validate our models on the original XNLI validation data (7500 examples per language), and we test the models on the original test data (15000 examples per language) in the validation set languages.

The idea to train and validate on the same sentences (in different languages) while testing on sentences from different treebanks (as we do for POS) or a different dataset split (as for XNLI) is to induce a slight distributional shift between validation and test data for the same language sample. This shift lets us evaluate the regularization strength of the gradient noise added by the DP-optimizer.

Training We employ the standard fine-tuning procedures for token classification (POS) and sequence classification (XNLI) proposed by Devlin et al. (2019). Similar to Li et al. (2021), we use DP-AdamW (i.e., the DP-SGD algorithm (Abadi et al., 2016) applied to the AdamW optimizer with default hyperparameters (Loshchilov and Hutter, 2019; Kingma and Ba, 2015)) to train with (ϵ, δ) -DP. We evaluate 6 different privacy budgets with $\epsilon \in \{1, 3, 8, 15, 30, \infty\}$.¹² We set $\delta = \frac{1e-4}{|D_{train}|}$ for POS, where $|D_{train}| = 7000$ is the length of the training dataset, and $\delta = 1e-6$ for XNLI.¹³ The noise multiplier σ corresponding to a particular (ϵ, δ) -budget is determined numerically before training through binary search. Our implementation builds upon the optimized Opacus (Yousefpour et al., 2021) privacy engine by Li et al. (2021).^{14,15} We use the Rényi differential privacy (RDP; Mironov, 2017; Mironov et al.,

2019) accountant with conversion to (ϵ, δ) -DP (Canonne et al., 2020). Hyper-parameter tuning on private data—which the POS and XNLI data in our study simulate—has been shown to incur additional privacy leakage (Liu and Talwar, 2019; Papernot and Steinke, 2021). Therefore, we try to keep hyper-parameter tuning to a minimum and rely on sensible priors to select a suitable range of hyper-parameters. For POS, we find that the range of good hyper-parameters for non-private settings transfers well to private settings if we just use slightly higher learning rates. For XNLI, we select hyper-parameters in a way that matches the sampling rate Li et al. (2021) found to suit the NLI tasks in the GLUE benchmark (Wang et al., 2018) well.¹⁶ Accordingly, we train with a maximum sequence length of 128 for 10 epochs with a total batch size of 96 for POS and 30 epochs with batch size 512 for XNLI.¹⁷ At each privacy budget, we train models (3 random initializations each) with 6 learning rates for POS ($1e-4, 3e-4, 5e-4, 7e-4, 1e-5, 5e-5, 7e-5, 1e-6$) and 3 learning rates for XNLI ($3e-4, 4e-4, 5e-4$ for private models and $9e-5, 1e-4, 2e-4$ for non-private models). Based on the validation accuracy we then select the 5 best settings for each privacy level and task, listed in Appendix C. The learning rate is linearly decayed after 50 warm-up steps for POS and without warm-up for XNLI. We perform gradient clipping (per-sample clipping in private settings) with a threshold of 0.1. Weight decay is set to 0.01.

Quantifying Multilingual Compression We present four metrics of multilingual compression: A common proxy task to measure the quality of cross-lingual representations is sentence retrieval (Artetxe and Schwenk, 2019; Dufter and Schütze, 2020; Libovický et al., 2020; Ravishankar and Søgaard, 2021; Liu et al., 2021b; Maronikolakis et al., 2021). Dufter and Schütze (2020) quantify the degree of multilingual compression using bidirectional sentence retrieval precision as follows:¹⁸

¹¹Regardless of test split size, each language contributes equally to the mean accuracy reported in Figure 2.

¹² $\epsilon = \infty$ refers to the standard, non-private setting.

¹³We deliberately use a larger δ for XNLI because it turned out to be much harder to achieve convergence than for POS. Even with the looser DP bounds from $\delta = 1e-6$, we were unable to find a hyper-parameter setting for $\epsilon = 1$ where the fine-tuned model was substantially better than random guessing.

¹⁴<https://github.com/lxuechen/private-transformers>

¹⁵We do not use ghost clipping, their proposed technique to fit larger batches on the GPU at the cost of training time, as we can still fit sufficiently large batches on our GPUs without.

¹⁶The sampling rate $q = \frac{B_{train}}{|D_{train}|}$, B denoting the batch size.

¹⁷Note that using fixed-size batches technically breaks the privacy guarantees of RDP based on the Sampled Gaussian Mechanism (Mironov et al., 2019). We follow the convention of using fixed-size batches, circumventing potential out-of-memory GPU issues, as a proxy for the true privacy spending and performance (see (Li et al., 2021) and Appendix D.4 in (Tramèr and Boneh, 2021)).

¹⁸Note that Dufter and Schütze (2020) also consider word alignment in their multilinguality score. We omit this task as it is not trivial to obtain ground truth alignments in our setup.

$$P = \frac{1}{2m} \sum_{i=1}^m \mathbb{1}_{\arg \max_k R_{ik}=i} + \mathbb{1}_{\arg \max_k R_{ki}=i}. \quad (1)$$

Here, $R \in \mathbb{R}^{m \times m}$ denotes the matrix of cosine similarities $R_{ij} = \cos(e_i^q, e_j^r)$ between the m sub-word representations e_i^q and e_j^r from a LM at indices i and j for a set of parallel sentences in the languages q and r .¹⁹

Kornblith et al. (2019) propose to use linear centered kernel alignment (CKA) as a similarity index for neural network representations. It is defined as

$$\text{CKA}(X, Y) = \frac{\|Y^T X\|_F^2}{\|X^T X\|_F \|Y^T Y\|_F}. \quad (2)$$

For LMs, the matrices X and Y are obtained by mean-pooling n sub-word representations at model layer l (Conneau et al., 2020b; Glavaš and Vulić, 2021). Typically, X and Y correspond to the representations from two different models for identical examples (Kornblith et al., 2019; Phang et al., 2021). We instead use the representations from a single model for a parallel sentence pair (s_q, s_r) in languages q and r as X and Y , respectively, to study the similarity of representations across languages, similar to Muller et al. (2021) and Conneau et al. (2020b). Anonymous (2022a) also use CKA as a metric of multilingual compression.

IsoScore (Rudman et al., 2021) is an isotropy metric that quantifies the degree to which a point cloud uniformly utilizes the vector space. In our context, this point cloud corresponds to the n mean-pooled sub-word representations at layer l . Prior work has shown that anisotropic representation spaces, such as the embedding spaces of large LMs (Ethayarajh, 2019), suffer from so-called *representation degeneration* (Gao et al., 2019), and that the isotropy of a model’s representation space correlates with its downstream task performance (Zhou et al., 2019; Wang et al., 2020; Zhou et al., 2021; Rajae and Pilehvar, 2021, *inter alia*). High isotropy also means languages are not compartmentalized and should therefore correlate with high compression. The IsoScore algorithm is outlined in Appendix D.

Representational similarity analysis (RSA; Kriegeskorte et al., 2008; Edelman, 1998) was originally introduced in the field of cognitive neuro-

science to analyze the similarity of fMRI activity patterns, but it is also applicable to neural network representations (Bouchacourt and Baroni, 2018; Chrupała, 2019; Chrupała and Alishahi, 2019; Lepori and McCoy, 2020; He et al., 2021, *inter alia*), e.g., to analyze their similarity across languages. RSA measures the similarity between the representational geometries (i.e., the arrangement in the vector space) of two sets of representations. The representational geometry is determined through pairwise (dis)similarity/distance metrics, and similarity is typically measured using a rank-based correlation metric such as Spearman’s ρ (Diedrichsen and Kriegeskorte, 2017).

Quantifying Instance-based Interpretability

Instance-based interpretability metrics can help us gain an understanding of the inner workings of a model (Koh and Liang, 2017; Yeh et al., 2018; Charpiat et al., 2019; Koh et al., 2019; Pruthi et al., 2020; Basu et al., 2020; K and Sjøgaard, 2021; Zhang et al., 2021; Kong and Chaudhuri, 2021, *inter alia*). Such metrics are approximations of leave-one-out-influence. Pruthi et al. (2020) proposed a both effective and practical method, called TracInCP,²⁰ to compute the influence of a training example z on the model’s prediction for another example z' , which could be a test example or z itself (called the self-influence). The influence is computed as follows:

$$\text{TracInCP}(z, z') = \sum_{i=1}^k \eta_i \nabla \ell(\theta_i, z) \cdot \nabla \ell(\theta_i, z'), \quad (3)$$

where η_i is the learning rate and $\nabla \ell(\theta_i, z)$ is the gradient of the loss w.r.t. the model parameters θ_i and inputs z for the i -th model checkpoint. We will use TracInCP as an approximation of interpretability in our experiments.

Evaluation We evaluate our models both during and after fine-tuning. For POS, we evaluate every 100 steps, and for XNLI, every 200 steps. We measure zero-shot cross-lingual transfer performance on the validation and test data by accuracy (token-level for POS and sequence-level for XNLI). To account for randomness, we take the mean of the best 5 seeds for each privacy budget.

The measures of multilingual compression (sentence retrieval precision, CKA, IsoScore, RSA) are

¹⁹The sub-word representations are taken from the LM’s layer l and mean-pooled over the sequence length (excluding special tokens).

²⁰“CP” stands for checkpoint; the method approximates TracInIdeal, which is impractical to compute, through model checkpoints taken during training (Pruthi et al., 2020).

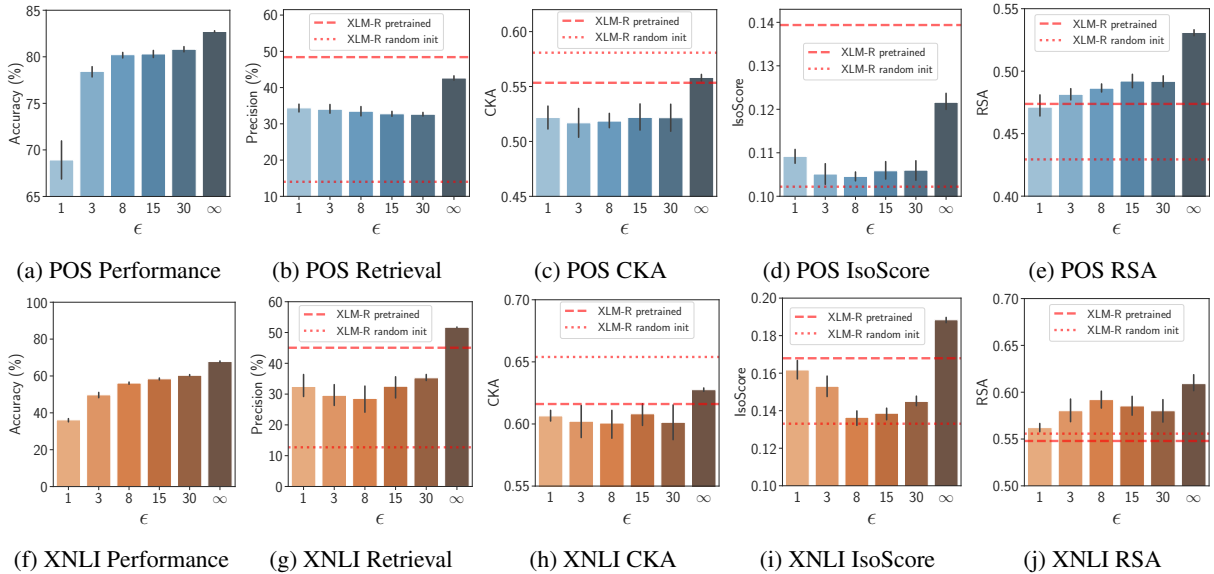


Figure 2: Task performance, sentence retrieval, CKA, IsoScore, and RSA results when fine-tuning with different privacy guarantees (∞ =non-private). We add the original pretrained XLM-R and XLM-R with randomly initialized weights for comparison. The results show how non-private fine-tuning balances multilingual compression and task performance. Strongly private fine-tuning ($\epsilon = 1$) is compatible with high compression (retrieval, CKA, IsoScore), but not with task performance. For medium levels of privacy (e.g., $\epsilon = 8$), we see the result of balancing privacy and task performance at the expense of multilingual compression.

394 computed using distinct evaluation corpora comprising parallel sentences for all possible language pairs in the respective training set language sample. For models trained on XNLI, we use 3000 sentence pairs per language pair from the TED 2020 corpus (Reimers and Gurevych, 2020) and 3500 pairs from the WikiMatrix dataset (Schwenk et al., 2021). For models trained for POS, we use 3500 pairs from TED 2020, 3500 pairs from WikiMatrix, and 900 pairs from Tatoeba,^{21,22,23} numbers chosen based on availability and memory constraints for the IsoScore computation.

406 Following Dufter and Schütze (2020), we evaluate the models at layers 0 and 8, which complement each other well with regard to the properties they capture, e.g., multilinguality and task-specificity (Choenni and Shutova, 2020; de Vries et al., 2020; Muller et al., 2021). We compute the sentence retrieval precision between language pairs and take the mean.²⁴ The IsoScore is computed for the contextualized representations of all examples in the

²¹<https://tatoeba.org>

²²We extract sentence pairs from Tatoeba using the tatoeba-tools library (<https://github.com/LBeaudoux/tatoebatools>).

²³We exclude TH from the WikiMatrix and Tatoeba evaluation sets for POS as there are insufficiently many sentence pairs available between TH and the remaining languages.

²⁴Sentence retrieval is bidirectional (see Eq. 1). Given $|L|$ languages, we therefore average over the full $\mathbb{R}^{|L| \times |L|}$ language pair matrix, only excluding the main diagonal.

415 respective corpus at once. In contrast, CKA and RSA scores are also computed per language pair, and then averaged across those.²⁵ For RSA, we use $D = 1 - \text{Spearman's } \rho$ and $S = \text{Spearman's } \rho$ as the dissimilarity and similarity metrics, respectively.²⁶ Finally, we average results for all four metrics across TED 2020, WikiMatrix, and Tatoeba, the two layers, and the 5 best seeds for each privacy budget. For comparison, we also compute all metrics for the original pretrained XLM-R model and for XLM-R with randomly initialized weights.

4 Results

426 **Privacy, Compression, Performance** We now empirically investigate the relationship between privacy, multilingual compression, and cross-lingual transfer performance. We present aggregated results in Figure 2 and non-aggregated results in Appendix F. We observe that the zero-shot accuracy decreases as we fine-tune with stronger privacy guarantees (Figures 2a and 2f), which is expected due to the *privacy-utility tradeoff* (Geng et al.,

²⁵CKA and RSA are symmetrical. Given $|L|$ languages, we thus only use the upper triangle of the $\mathbb{R}^{|L| \times |L|}$ language pair matrix, still excluding the main diagonal.

²⁶This is consistent with (Zhelezniak et al., 2019) and (Lepori and McCoy, 2020) who show that Spearman's ρ is more suitable for RSA with embeddings than conventional similarity metrics such as cosine similarity.

2020). In particular, the relatively small sizes of our training datasets make private LM fine-tuning more challenging (Kerrigan et al., 2020; Habernal, 2021; Senge et al., 2021; Yu et al., 2021) because, for a fixed number of update steps, the gradient noise added per update step grows as the size of the training dataset decreases (Tramèr and Boneh, 2021; McMahan et al., 2018). Note although the private models tend to underperform the non-private models by a large margin on the validation set (>30% for XNLI, as shown in Appendix Table 6), the performance gap on the test set is noticeably smaller, which shows that training with differential privacy, like other noise injection schemes (Bishop, 1995), is also a form of regularization.

Figures 2b and 2g display sentence retrieval precision when fine-tuning with different privacy budgets. The highest compression is achieved by the non-private models. The second-highest compression is achieved for $\epsilon = 1$, our most private models. Both suggest non-linear privacy–compression interactions, with POS showing lowest compression for $\epsilon = 30$ (or higher) and XNLI showing lowest compression for $\epsilon = 8$. The results are very similar for IsoScore (Figures 2d, 2i) and also similar, albeit less pronounced for CKA (Figures 2c, 2h).²⁷ RSA, in contrast, exhibits very low scores for highly private models; see Appendix E for an explanation.

Overall, these results show that we can achieve *strong compression and strong performance at the cost of privacy* ($\epsilon = \infty$), *strong compression and strong privacy at the cost of performance* ($\epsilon = 1$), or *trade-off performance and privacy at the cost of compression* (e.g., $\epsilon = 8$). At first thought, it may seem counter-intuitive that multilingual compression and cross-lingual transfer performance are not strictly correlated. However, in the fine-tuning setting, it is possible to disregard all task-specific knowledge in favor of multilingual compression, which ultimately leads to poor performance. Vice-versa, a model may exploit spurious correlations in the data to make correct predictions without actually relying on cross-lingual signal. An example for the former case is the pretrained (but not fine-tuned) XLM-R model, which scores highly in

²⁷Note the randomly initialized XLM-R model scores particularly highly in CKA. This phenomenon is explained by the high dimensionality ($d = 768$) of the contextualized representations, considering that CKA saturates with increasing network width (Kornblith et al., 2019), and the high centroid similarity of random activations.

multilingual compression (as displayed in Figure 2) but has poor cross-lingual transfer performance in the downstream tasks.

We also find that in some fine-tuning settings, e.g., $\epsilon = \infty$, the multilingual compression surpasses that of the pretrained XLM-R. While Liu et al. (2021b) have previously shown that sentence retrieval performance typically drops (i.e., compression worsens) over the course of fine-tuning (which we confirm in Appendix Fig. 4), this finding clearly shows that there are exceptions. Future work may investigate this further.

Lastly, sentence retrieval and CKA scores are always highest between typologically similar languages and languages over-represented in pretraining (see Table 1 for a comparison across all languages) *across all levels of privacy*, as shown by the non-aggregated results in the Appendix Figures 5–12. This finding thus extends conclusions from prior work (Pires et al., 2019; Wu and Dredze, 2019; K et al., 2020; Lauscher et al., 2020) to private models.

5 Are more multilingual models less interpretable?

Metric To answer this question, we introduce a new metric, termed InfU (**I**nfluence **U**niformity), which is based on the TracInCP influence scores for each training example in the (multi-)parallel dataset $D = \{\dots, i_1, \dots, i_{|L|}, \dots\}$, where i_j and i_k are translation equivalents. As its name suggests, InfU is a measure of uniformity, based on the idea that for a perfectly multilingual model, the following equation should hold $\forall j, k, q, r \in L$:

$$\text{TracInCP}(i_j, i_k) = \text{TracInCP}(i_q, i_r) \quad (4)$$

We compute InfU for a model \mathcal{M} and the set of translation equivalent examples $i = \{i_1, \dots, i_{|L|}\}$ as

$$\text{InfU}_{\mathcal{M}}(i) = \frac{1}{|L|} \sum_k^{|L|} H(\sigma(\text{TracInCP}(i_k, i))), \quad (5)$$

where H is the entropy with $\log_{|L|}$ and σ is a softmax used to obtain a probability distribution over the list of influence scores. InfU is maximized (InfU = 1) for uniform influence scores, fulfilling Eq. 4. In this scenario of maximum uncertainty our model is also the least interpretable because we do not know the languages of the most or least influential examples for another example’s prediction.

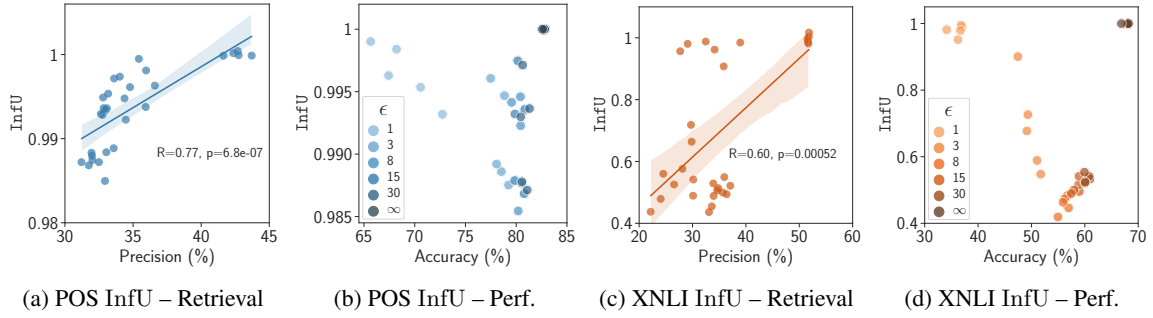


Figure 3: Linear fit and Pearson correlation between the influence uniformity InfU and sentence retrieval precision (3a, 3c) and InfU versus downstream performance for different levels of privacy (3b, 3d). We see significant positive correlations between retrieval precision and InfU, suggesting a negative correlation between multilingual compression and interpretability. For task performance, we see the trade-off between interpretability (InfU) and privacy, which aligns with our theoretical expectations (§2).

While it essentially follows from the above definition that multilingual compression and interpretability are at odds, we use it to study to what extent interpretability aligns with privacy, our metrics used in §4, and cross-lingual transfer performance.

Setup We use 1000 examples from the respective training dataset for both POS and XNLI. We use the last 3 model checkpoints with their corresponding learning rates to compute TraInCP scores.²⁸ Checkpoints were stored every 100 training steps. We use the gradients w.r.t. all model parameters.

Results and Analysis We plot the mean InfU against the mean sentence retrieval precision for our fine-tuned models and compute Pearson’s R in Figures 3a and 3c. For both tasks, there is a significant ($p < 0.05$) strong positive correlation between the InfU score and the multilingual compression as determined through sentence retrieval. This result further supports the idea that *multilingual compression is at odds with interpretability*.

We also see that highly private and correspondingly low-performing models score highly in InfU (Figures 3b, 3d), which suggests that they are not interpretable. The same applies to the non-private and correspondingly high-performing models. For medium levels of privacy we, again, see a trade-off characterized by lower InfU, i.e., better interpretability, and medium performance. It thus also becomes clear that, unless optimizing for them jointly, *high privacy, interpretability, and performance are not compatible*, because the high-performing models are strictly low in privacy and interpretability and the models high in privacy are

strictly low in performance and interpretability. We can at best achieve a satisfactory trade-off between these three objectives.

6 Conclusion

In this work, we conducted a preliminary investigation of the interactions between multilingual compression, privacy, interpretability, and fairness in the context of multilingual language models. We first found, through theoretical exploration, that privacy and interpretability are generally incompatible, both inside and outside the multilingual space. We also established that privacy and fairness, although often thought to be fundamentally at odds, are theoretically compatible in the multilingual space.

We further explored the space empirically. Our results overall support the theoretical expectations we laid out; we found that high multilingual compression can be achieved either by optimizing for performance or by optimizing for privacy. Likewise, by trading off privacy and performance, we compromise multilingual compression. In other words, the interactions between these objectives are non-linear. Ideally, however, we want models to do well in all of these dimensions, which remains an open problem. We hope that our study will spark future research in this direction.

Finally, we introduced a new metric, the influence uniformity, to empirically validate the theoretical idea that privacy and interpretability are incompatible and that the interactions between privacy, interpretability, and multilingual compression are, therefore, also non-linear.

²⁸Since the learning rate changes constantly, we use the learning rate from the end of each checkpointing interval.

7 Ethical Aspects and Broader Impact

Beyond performance metrics, it is crucial to study objectives such as privacy, interpretability, and fairness in (multilingual) NLP. Our work aims to provide a starting point for further research in this area. Our empirical investigation, including the models we train, fully relies on publicly available models and data. Moreover, we do not create any new datasets. Therefore, we see practically no potential for misuse of the results of our work.

References

- Martín Abadi, Andy Chu, Ian J. Goodfellow, H. Brendan McMahan, Ilya Mironov, Kunal Talwar, and Li Zhang. 2016. [Deep learning with differential privacy](#). In *Proceedings of the 2016 ACM SIGSAC Conference on Computer and Communications Security*, pages 308–318, Vienna, Austria. ACM.
- Sushant Agarwal. 2021. [Trade-offs between fairness and privacy in machine learning](#). In *IJCAI 2021 Workshop on AI for Social Good*. International Joint Conference of Artificial Intelligence (IJCAI).
- Anonymous. 2022a. [Enhancing cross-lingual transfer by manifold mixup](#). In *Submitted to the 10th International Conference on Learning Representations (ICLR)*. Under review.
- Anonymous. 2022b. [Fairness in representation for multilingual NLP: Insights from controlled experiments on conditional language modeling](#). In *Submitted to the 10th International Conference on Learning Representations (ICLR)*. Under review.
- Mikel Artetxe and Holger Schwenk. 2019. [Massively multilingual sentence embeddings for zero-shot cross-lingual transfer and beyond](#). *Transactions of the Association for Computational Linguistics*, 7:597–610.
- Eugene Bagdasaryan, Omid Poursaeed, and Vitaly Shmatikov. 2019. [Differential privacy has disparate impact on model accuracy](#). In *Advances in Neural Information Processing Systems 32: Annual Conference on Neural Information Processing Systems (NeurIPS)*, pages 15453–15462, Vancouver, BC, Canada. Curran Associates, Inc.
- Samyadeep Basu, Xuchen You, and Soheil Feizi. 2020. [On second-order group influence functions for black-box predictions](#). In *Proceedings of the 37th International Conference on Machine Learning (ICML)*, volume 119 of *Proceedings of Machine Learning Research*, pages 715–724, Online. PMLR.
- Chris M. Bishop. 1995. [Training with noise is equivalent to tikhonov regularization](#). *Neural Computation*, 7(1):108–116.

- Diane Bouchacourt and Marco Baroni. 2018. [How agents see things: On visual representations in an emergent language game](#). In *Proceedings of the 2018 Conference on Empirical Methods in Natural Language Processing*, pages 981–985, Brussels, Belgium. Association for Computational Linguistics.
- Clément L. Canonne, Gautam Kamath, and Thomas Steinke. 2020. [The discrete gaussian for differential privacy](#). In *Advances in Neural Information Processing Systems 33: Annual Conference on Neural Information Processing Systems (NeurIPS)*, pages 15676–15688, Online. Curran Associates, Inc.
- Guillaume Charpiat, Nicolas Girard, Loris Felardos, and Yuliya Tarabalka. 2019. [Input similarity from the neural network perspective](#). In *Advances in Neural Information Processing Systems 32: Annual Conference on Neural Information Processing Systems (NeurIPS)*, pages 5343–5352, Vancouver, BC, Canada. Curran Associates, Inc.
- Rochelle Choenni and Ekaterina Shutova. 2020. [What does it mean to be language-agnostic? probing multilingual sentence encoders for typological properties](#). *arXiv preprint*.
- Monojit Choudhury and Amit Deshpande. 2021. [How linguistically fair are multilingual pre-trained language models?](#) In *Proceedings of the 35th AAAI Conference on Artificial Intelligence*, pages 12710–12718, Online. AAAI Press.
- Grzegorz Chrupała. 2019. [Symbolic inductive bias for visually grounded learning of spoken language](#). In *Proceedings of the 57th Annual Meeting of the Association for Computational Linguistics*, pages 6452–6462, Florence, Italy. Association for Computational Linguistics.
- Grzegorz Chrupała and Afra Alishahi. 2019. [Correlating neural and symbolic representations of language](#). In *Proceedings of the 57th Annual Meeting of the Association for Computational Linguistics*, pages 2952–2962, Florence, Italy. Association for Computational Linguistics.
- Alexis Conneau, Kartikay Khandelwal, Naman Goyal, Vishrav Chaudhary, Guillaume Wenzek, Francisco Guzmán, Edouard Grave, Myle Ott, Luke Zettlemoyer, and Veselin Stoyanov. 2020a. [Unsupervised cross-lingual representation learning at scale](#). In *Proceedings of the 58th Annual Meeting of the Association for Computational Linguistics*, pages 8440–8451, Online. Association for Computational Linguistics.
- Alexis Conneau, Ruty Rinott, Guillaume Lample, Adina Williams, Samuel Bowman, Holger Schwenk, and Veselin Stoyanov. 2018. [XNLI: Evaluating cross-lingual sentence representations](#). In *Proceedings of the 2018 Conference on Empirical Methods in Natural Language Processing*, pages 2475–2485, Brussels, Belgium. Association for Computational Linguistics.

702	Alexis Conneau, Shijie Wu, Haoran Li, Luke Zettlemoyer, and Veselin Stoyanov. 2020b. Emerging cross-lingual structure in pretrained language models . In <i>Proceedings of the 58th Annual Meeting of the Association for Computational Linguistics</i> , pages 6022–6034, Online. Association for Computational Linguistics.	758
703		759
704		760
705		761
706		762
707		
708		
709	Wietse de Vries, Andreas van Cranenburgh, and Malvina Nissim. 2020. What’s so special about BERT’s layers? a closer look at the NLP pipeline in monolingual and multilingual models . In <i>Findings of the Association for Computational Linguistics: EMNLP 2020</i> , pages 4339–4350, Online. Association for Computational Linguistics.	763
710		764
711		765
712		766
713		767
714		768
715		
716	Jacob Devlin, Ming-Wei Chang, Kenton Lee, and Kristina Toutanova. 2019. BERT: Pre-training of deep bidirectional transformers for language understanding . In <i>Proceedings of the 2019 Conference of the North American Chapter of the Association for Computational Linguistics: Human Language Technologies, Volume 1 (Long and Short Papers)</i> , pages 4171–4186, Minneapolis, Minnesota. Association for Computational Linguistics.	769
717		770
718		771
719		772
720		773
721		774
722		775
723		
724		
725	Jörn Diedrichsen and Nikolaus Kriegeskorte. 2017. Representational models: A common framework for understanding encoding, pattern-component, and representational-similarity analysis . <i>PLOS Computational Biology</i> , 13(4):1–33.	776
726		777
727		778
728		779
729		780
730	Philipp Dufter and Hinrich Schütze. 2020. Identifying elements essential for BERT’s multilinguality . In <i>Proceedings of the 2020 Conference on Empirical Methods in Natural Language Processing (EMNLP)</i> , pages 4423–4437, Online. Association for Computational Linguistics.	781
731		782
732		
733		
734		
735		
736	Cynthia Dwork. 2006. Differential privacy . In <i>Proceedings of the 33rd International Colloquium on Automata, Languages and Programming (ICALP), Part II</i> , volume 4052 of <i>Lecture Notes in Computer Science</i> , pages 1–12, Venice, Italy. Springer.	783
737		784
738		785
739		786
740		787
741	Cynthia Dwork, Frank McSherry, Kobbi Nissim, and Adam Smith. 2006. Calibrating noise to sensitivity in private data analysis . In <i>Proceedings of the 3rd Conference on Theory of Cryptography (TCC)</i> , page 265–284, Berlin / Heidelberg, Germany. Springer-Verlag.	788
742		789
743		790
744		791
745		792
746		793
747	Cynthia Dwork and Aaron Roth. 2014. The algorithmic foundations of differential privacy . <i>Foundations and Trends in Theoretical Computer Science</i> , 9(3-4):211–407.	794
748		795
749		796
750		797
751	Shimon Edelman. 1998. Representation is representation of similarities . <i>Behavioral and Brain Sciences</i> , 21(4):449–467.	798
752		799
753		800
754	Kawin Ethayarajh. 2019. How contextual are contextualized word representations? Comparing the geometry of BERT, ELMo, and GPT-2 embeddings . In <i>Proceedings of the 2019 Conference on Empirical Methods in Natural Language Processing and the 9th International Joint Conference on Natural Language Processing (EMNLP-IJCNLP)</i> , pages 55–65, Hong Kong, China. Association for Computational Linguistics.	801
755		802
756		803
757		804
		805
		806
		807
		808
		809
		810
		811
		812
		813
		814

815	Karthikeyan K, Zihan Wang, Stephen Mayhew, and Dan Roth. 2020. Cross-lingual ability of multilingual BERT: an empirical study . In <i>Proceedings of the 8th International Conference on Learning Representations (ICLR)</i> , Online. OpenReview.net.	871
816		872
817		873
818		
819		
820	Gavin Kerrigan, Dylan Slack, and Jens Tuyls. 2020. Differentially private language models benefit from public pre-training . In <i>Proceedings of the Second Workshop on Privacy in NLP</i> , pages 39–45, Online. Association for Computational Linguistics.	874
821		875
822		876
823		877
824		878
825	Muhammad Khalifa, Muhammad Abdul-Mageed, and Khaled Shaalan. 2021. Self-training pre-trained language models for zero- and few-shot multi-dialectal Arabic sequence labeling . In <i>Proceedings of the 16th Conference of the European Chapter of the Association for Computational Linguistics: Main Volume</i> , pages 769–782, Online. Association for Computational Linguistics.	879
826		880
827		
828		
829		
830		
831		
832		
833	Diederik P. Kingma and Jimmy Ba. 2015. Adam: A method for stochastic optimization . In <i>Proceedings of the 3rd International Conference on Learning Representations (ICLR)</i> , San Diego, CA, USA.	881
834		882
835		883
836		884
837	Pang Wei Koh, Kai-Siang Ang, Hubert H. K. Teo, and Percy Liang. 2019. On the accuracy of influence functions for measuring group effects . In <i>Advances in Neural Information Processing Systems 32: Annual Conference on Neural Information Processing Systems (NeurIPS)</i> , pages 5255–5265, Vancouver, BC, Canada. Curran Associates, Inc.	885
838		886
839		887
840		888
841		889
842		890
843		891
844	Pang Wei Koh and Percy Liang. 2017. Understanding black-box predictions via influence functions . In <i>Proceedings of the 34th International Conference on Machine Learning (ICML)</i> , volume 70 of <i>Proceedings of Machine Learning Research</i> , pages 1885–1894, Sydney, NSW, Australia. PMLR.	892
845		893
846		894
847		895
848		896
849		897
850	Zhifeng Kong and Kamalika Chaudhuri. 2021. Understanding instance-based interpretability of variational auto-encoders . In <i>Advances in Neural Information Processing Systems 34: Annual Conference on Neural Information Processing Systems (NeurIPS)</i> , Online. Curran Associates, Inc.	898
851		899
852		900
853		
854		
855		
856	Simon Kornblith, Mohammad Norouzi, Honglak Lee, and Geoffrey Hinton. 2019. Similarity of neural network representations revisited . In <i>Proceedings of the 36th International Conference on Machine Learning (ICML)</i> , volume 97 of <i>Proceedings of Machine Learning Research</i> , pages 3519–3529, Long Beach, CA, USA. PMLR.	901
857		902
858		903
859		904
860		905
861		906
862		
863	Nikolaus Kriegeskorte, Marieke Mur, and Peter Bannettini. 2008. Representational similarity analysis - connecting the branches of systems neuroscience . <i>Frontiers in Systems Neuroscience</i> , 2:4.	907
864		908
865		909
866		910
867	Anne Lauscher, Vinit Ravishankar, Ivan Vulić, and Goran Glavaš. 2020. From zero to hero: On the limitations of zero-shot language transfer with multilingual Transformers . In <i>Proceedings of the 2020 Conference on Empirical Methods in Natural Language Processing (EMNLP)</i> , pages 4483–4499, Online. Association for Computational Linguistics.	911
868		912
869		913
870		914
		915
		916
		917
		918
		919
		920
		921
		922
		923
		924
		925
		926
		927
		928

929	Lingjuan Lyu, Xuanli He, and Yitong Li. 2020. Differentially private representation for NLP: Formal guarantee and an empirical study on privacy and fairness . In <i>Findings of the Association for Computational Linguistics: EMNLP 2020</i> , pages 2355–2365, Online. Association for Computational Linguistics.	984
930		985
931		986
932		987
933		988
934		989
935	Antonis Maronikolakis, Philipp Dufter, and Hinrich Schütze. 2021. Wine is not v i n. on the compatibility of tokenizations across languages . In <i>Findings of the Association for Computational Linguistics: EMNLP 2021</i> , pages 2382–2399, Punta Cana, Dominican Republic. Association for Computational Linguistics.	990
936		991
937		992
938		993
939		994
940		995
941	H. Brendan McMahan, Daniel Ramage, Kunal Talwar, and Li Zhang. 2018. Learning differentially private recurrent language models . In <i>Proceedings of the 6th International Conference on Learning Representations (ICLR)</i> , Vancouver, BC, Canada. OpenReview.net.	996
942		997
943		998
944		999
945		1000
946		1001
947	Ilya Mironov. 2017. Rényi differential privacy . In <i>30th IEEE Computer Security Foundations Symposium (CSF)</i> , pages 263–275, Santa Barbara, CA, USA. IEEE Computer Society.	1002
948		1003
949		1004
950		1005
951	Ilya Mironov, Kunal Talwar, and Li Zhang. 2019. Rényi differential privacy of the sampled gaussian mechanism . <i>arXiv preprint</i> .	1006
952		1007
953		1008
954	Benjamin Muller, Yanai Elazar, Benoît Sagot, and Djamé Seddah. 2021. First align, then predict: Understanding the cross-lingual ability of multilingual BERT . In <i>Proceedings of the 16th Conference of the European Chapter of the Association for Computational Linguistics: Main Volume</i> , pages 2214–2231, Online. Association for Computational Linguistics.	1009
955		1010
956		1011
957		1012
958		1013
959		1014
960		1015
961	Rakshit Naidu, Aman Priyanshu, Aadith Kumar, Sasikanth Kotti, Haofan Wang, and Fatemehsadat Mireshghallah. 2021. When differential privacy meets interpretability: A case study . In <i>CVPR 2021 Workshop for Responsible Computer Vision (RCV)</i> .	1016
962		1017
963		1018
964		1019
965		1020
966	Joakim Nivre, Marie-Catherine de Marneffe, Filip Ginter, Jan Hajič, Christopher D. Manning, Sampo Pyysalo, Sebastian Schuster, Francis Tyers, and Daniel Zeman. 2020. Universal Dependencies v2: An evergrowing multilingual treebank collection . In <i>Proceedings of the 12th Language Resources and Evaluation Conference</i> , pages 4034–4043, Marseille, France. European Language Resources Association.	1021
967		1022
968		1023
969		1024
970		1025
971		1026
972		1027
973		1028
974	Marlotte Pannekoek and Giacomo Spigler. 2021. Investigating trade-offs in utility, fairness and differential privacy in neural networks . <i>arXiv preprint</i> .	1029
975		1030
976		1031
977	Nicolas Papernot and Thomas Steinke. 2021. Hyperparameter tuning with renyi differential privacy . <i>arXiv preprint</i> .	1032
978		1033
979		1034
980	Adam Paszke, Sam Gross, Francisco Massa, Adam Lerer, James Bradbury, Gregory Chanan, Trevor Killeen, Zeming Lin, Natalia Gimelshein, Luca Antiga, Alban Desmaison, Andreas Köpf, Edward Z.	1035
981		1036
982		1037
983		1038
	Yang, Zachary DeVito, Martin Raison, Alykhan Tejani, Sasank Chilamkurthy, Benoit Steiner, Lu Fang, Junjie Bai, and Soumith Chintala. 2019. Pytorch: An imperative style, high-performance deep learning library . In <i>Advances in Neural Information Processing Systems 32: Annual Conference on Neural Information Processing Systems (NeurIPS)</i> , pages 8024–8035, Vancouver, BC, Canada. Curran Associates, Inc.	1039
		1040
	Jason Phang, Haokun Liu, and Samuel R. Bowman. 2021. Fine-tuned transformers show clusters of similar representations across layers . In <i>Proceedings of the Fourth BlackboxNLP Workshop on Analyzing and Interpreting Neural Networks for NLP</i> , pages 529–538, Punta Cana, Dominican Republic. Association for Computational Linguistics.	1041
		1042
	Telmo Pires, Eva Schlinger, and Dan Garrette. 2019. How multilingual is multilingual BERT? In <i>Proceedings of the 57th Annual Meeting of the Association for Computational Linguistics</i> , pages 4996–5001, Florence, Italy. Association for Computational Linguistics.	1043
		1044
	Yada Pruksachatkun, Anil Ramakrishna, Kai-Wei Chang, Satyapriya Krishna, Jwala Dhamala, Tanaya Guha, and Xiang Ren, editors. 2021. <i>Proceedings of the First Workshop on Trustworthy Natural Language Processing</i> . Association for Computational Linguistics, Online.	1045
		1046
	Garima Pruthi, Frederick Liu, Satyen Kale, and Mukund Sundararajan. 2020. Estimating training data influence by tracing gradient descent . In <i>Advances in Neural Information Processing Systems 33: Annual Conference on Neural Information Processing Systems (NeurIPS)</i> , Online. Curran Associates, Inc.	1047
		1048
	Sara Rajae and Mohammad Taher Pilehvar. 2021. A cluster-based approach for improving isotropy in contextual embedding space . In <i>Proceedings of the 59th Annual Meeting of the Association for Computational Linguistics and the 11th International Joint Conference on Natural Language Processing (Volume 2: Short Papers)</i> , pages 575–584, Online. Association for Computational Linguistics.	1049
		1050
	Vinit Ravishankar and Anders Søgaard. 2021. The impact of positional encodings on multilingual compression . In <i>Proceedings of the 2021 Conference on Empirical Methods in Natural Language Processing</i> , pages 763–777, Online and Punta Cana, Dominican Republic. Association for Computational Linguistics.	1051
		1052
	Nils Reimers and Iryna Gurevych. 2020. Making monolingual sentence embeddings multilingual using knowledge distillation . In <i>Proceedings of the 2020 Conference on Empirical Methods in Natural Language Processing (EMNLP)</i> , pages 4512–4525, Online. Association for Computational Linguistics.	1053
		1054
	William Rudman, Nate Gillman, Taylor Rayne, and Carsten Eickhoff. 2021. IsoScore: Measuring the uniformity of vector space utilization . <i>arXiv preprint</i> .	1055

1041	Holger Schwenk, Vishrav Chaudhary, Shuo Sun, Hongyu Gong, and Francisco Guzmán. 2021. Wiki-Matrix: Mining 135M parallel sentences in 1620 language pairs from Wikipedia . In <i>Proceedings of the 16th Conference of the European Chapter of the Association for Computational Linguistics: Main Volume</i> , pages 1351–1361, Online. Association for Computational Linguistics.	1099
1042		1100
1043		1101
1044		1102
1045		1103
1046		1104
1047		1105
1048		1106
1049	Ramprasaath R. Selvaraju, Michael Cogswell, Abhishek Das, Ramakrishna Vedantam, Devi Parikh, and Dhruv Batra. 2019. Grad-cam: Visual explanations from deep networks via gradient-based localization . <i>International Journal of Computer Vision</i> , 128(2):336–359.	1107
1050		1108
1051		1109
1052		1110
1053		1111
1054		1112
1055	Manuel Senge, Timour Igamberdiev, and Ivan Habernal. 2021. One size does not fit all: Investigating strategies for differentially-private learning across nlp tasks . <i>arXiv preprint</i> .	1113
1056		1114
1057		
1058		
1059	Jasdeep Singh, Bryan McCann, Richard Socher, and Caiming Xiong. 2019. BERT is not an interlingua and the bias of tokenization . In <i>Proceedings of the 2nd Workshop on Deep Learning Approaches for Low-Resource NLP (DeepLo 2019)</i> , pages 47–55, Hong Kong, China. Association for Computational Linguistics.	1115
1060		1116
1061		1117
1062		1118
1063		1119
1064		1120
1065		1121
1066	Florian Tramèr and Dan Boneh. 2021. Differentially private learning needs better features (or much more data) . In <i>Proceedings of the 9th International Conference on Learning Representations (ICLR)</i> , Online. OpenReview.net.	1122
1067		1123
1068		1124
1069		1125
1070		1126
1071	Alex Wang, Amanpreet Singh, Julian Michael, Felix Hill, Omer Levy, and Samuel Bowman. 2018. GLUE: A multi-task benchmark and analysis platform for natural language understanding . In <i>Proceedings of the 2018 EMNLP Workshop BlackboxNLP: Analyzing and Interpreting Neural Networks for NLP</i> , pages 353–355, Brussels, Belgium. Association for Computational Linguistics.	1127
1072		1128
1073		
1074		
1075		
1076		
1077		
1078		
1079	Cindy Wang and Michele Banko. 2021. Practical transformer-based multilingual text classification . In <i>Proceedings of the 2021 Conference of the North American Chapter of the Association for Computational Linguistics: Human Language Technologies: Industry Papers</i> , pages 121–129, Online. Association for Computational Linguistics.	1129
1080		1130
1081		1131
1082		1132
1083		1133
1084		1134
1085		
1086	Jialu Wang, Yang Liu, and Xin Eric Wang. 2021. Assessing multilingual fairness in pre-trained multimodal representations . <i>arXiv preprint</i> .	1135
1087		1136
1088		1137
1089	Lingxiao Wang, Jing Huang, Kevin Huang, Ziniu Hu, Guangtao Wang, and Quanquan Gu. 2020. Improving neural language generation with spectrum control . In <i>Proceedings of the 8th International Conference on Learning Representations (ICLR)</i> , Online. OpenReview.net.	1138
1090		1139
1091		1140
1092		1141
1093		1142
1094		1143
1095	Thomas Wolf, Lysandre Debut, Victor Sanh, Julien Chaumond, Clement Delangue, Anthony Moi, Pierric Cistac, Tim Rault, Remi Louf, Morgan Funtowicz, Joe Davison, Sam Shleifer, Patrick von Platen, Clara Ma, Yacine Jernite, Julien Plu, Canwen Xu, Teven Le Scao, Sylvain Gugger, Mariama Drame, Quentin Lhoest, and Alexander Rush. 2020. Transformers: State-of-the-art natural language processing . In <i>Proceedings of the 2020 Conference on Empirical Methods in Natural Language Processing: System Demonstrations</i> , pages 38–45, Online. Association for Computational Linguistics.	1144
1096		1145
1097		1146
1098		1147
		1148
		1149
		1150
		1151
		1152
		1153
		1154
		1155
		1156
		1157

1158	Cassidy, Tatiana Cavalcanti, Gülşen Cebiroğlu Eryiğit, Flavio Massimiliano Cecchini, Giuseppe G. A. Celano, Slavomír Čéplö, Neslihan Cesur, Savas Cetin, Özlem Çetinoğlu, Fabricio Chalub, Shweta Chauhan, Ethan Chi, Taishi Chika, Yongseok Cho, Jinho Choi, Jayeol Chun, Alessandra T. Cignarella, Silvie Cinková, Aurélie Collomb, Çağrı Çöltekin, Miriam Connor, Marine Courtin, Mihaela Cristescu, Philemon. Daniel, Elizabeth Davidson, Marie-Catherine de Marneffe, Valeria de Paiva, Mehmet Oguz Derin, Elvis de Souza, Arantza Diaz de Ilarraza, Carly Dickerson, Arawinda Dinakaramani, Elisa Di Nuovo, Bamba Dione, Peter Dirix, Kaja Dobrovoljc, Timothy Dozat, Kira Droganova, Puneet Dwivedi, Hanne Eckhoff, Sandra Eiche, Marhaba Eli, Ali Elkahky, Binyam Ephrem, Olga Erina, Tomaz Erjavec, Aline Etienne, Wograine Evelyn, Sidney Facundes, Richárd Farkas, Marília Fernanda, Hector Fernandez Alcalde, Jennifer Foster, Cláudia Freitas, Kazunori Fujita, Katarína Gajdošová, Daniel Galbraith, Marcos Garcia, Moa Gårdenfors, Sebastian Garza, Fabrício Ferraz Gerardi, Kim Gerdes, Filip Ginter, Gustavo Godoy, Iakes Goenaga, Koldo Gojenola, Memduh Gökırmak, Yoav Goldberg, Xavier Gómez Guinovart, Berta González Saavedra, Bernadeta Griciūtė, Matias Grioni, Loïc Grobol, Normunds Grūzītis, Bruno Guillaume, Céline Guillot-Barbance, Tunga Güngör, Nizar Habash, Hinrik Hafsteinsson, Jan Hajič, Jan Hajič jr., Mika Hämäläinen, Linh Hà Mỹ, Na-Rae Han, Muhammad Yudistira Hanifmuti, Sam Hardwick, Kim Harris, Dag Haug, Johannes Heinicke, Oliver Hellwig, Felix Hennig, Barbora Hladká, Jaroslava Hlaváčová, Florinel Hociung, Petter Hohle, Eva Huber, Jena Hwang, Takumi Ikeda, Anton Karl Ingason, Radu Ion, Elena Irimia, Qlájídé Ishola, Kaoru Ito, Tomáš Jelínek, Apoorva Jha, Anders Johannsen, Hildur Jónsdóttir, Fredrik Jørgensen, Markus Juutinen, Sarveswaran K, Hüner Kaşıkara, Andre Kaasen, Nadezhda Kabaeva, Sylvain Kahane, Hiroshi Kanayama, Jenna Kanerva, Neslihan Kara, Boris Katz, Tolga Kayadelen, Jessica Kenney, Václava Kettnerová, Jesse Kirchner, Elena Klementieva, Arne Köhn, Abdullatif Köksal, Kamil Kopacewicz, Timo Korkiakangas, Natalia Kotsyba, Jolanta Kovalevskaitė, Simon Krek, Parameswari Krishnamurthy, Oğuzhan Kuyrukçu, Aslı Kuzgun, Sookyoung Kwak, Veronika Laippala, Lucia Lam, Lorenzo Lambertino, Tatiana Lando, Septina Dian Larasati, Alexei Lavrentiev, John Lee, Phuong Lê Hồng, Alessandro Lenci, Saran Lertpradit, Herman Leung, Maria Levina, Cheuk Ying Li, Josie Li, Keying Li, Yuan Li, KyungTae Lim, Bruna Lima Padovani, Krister Lindén, Nikola Ljubešić, Olga Loginova, Andry Luthfi, Mikko Luukko, Olga Lyashevskaya, Teresa Lynn, Vivien Macketanz, Aibek Makazhanov, Michael Mandl, Christopher Manning, Ruli Manurung, Büşra Marşan, Cătălina Mărănduc, David Mareček, Katrin Marheinecke, Héctor Martínez Alonso, André Martins, Jan Mašek, Hiroshi Matsuda, Yuji Matsumoto, Alessandro Mazzei, Ryan McDonald, Sarah McGuinness, Gustavo Mendonça, Niko Miekka, Karina Mischenkova, Margarita Misirpashayeva, Anna Missilä, Cătălin Mi-	titelu, Maria Mitrofan, Yusuke Miyao, AmirHossein Mojiri Foroushani, Judit Molnár, Amirsaeid Moloodi, Simonetta Montemagni, Amir More, Laura Moreno Romero, Giovanni Moretti, Keiko Sophie Mori, Shinsuke Mori, Tomohiko Morioka, Shigeki Moro, Bjartur Mortensen, Bohdan Moskalevskyi, Kadri Muischnek, Robert Munro, Yugo Murawaki, Kaili Müürisep, Pinkey Nainwani, Mariam Nakhlé, Juan Ignacio Navarro Horñiacek, Anna Nedoluzhko, Gunta Nešpore-Bērkalne, Manuela Nevaci, Lương Nguyễn Thị, Huyền Nguyễn Thị Minh, Yoshihiro Nikaïdo, Vitaly Nikolaev, Rattima Nitisaroj, Alireza Nourian, Hanna Nurmi, Stina Ojala, Atul Kr. Ojha, Adédayò Oluókun, Mai Omura, Emeka Onwuegbuzia, Petya Osenova, Robert Östling, Lilja Øvrelið, Şaziye Betül Özateş, Merve Özçelik, Arzucan Özgür, Balkız Öztürk Başaran, Hyunji Hayley Park, Niko Partanen, Elena Pascual, Marco Passarotti, Agnieszka Patejuk, Guilherme Paulino-Passos, Angelika Peljak-Łapińska, Siyao Peng, Cene-Augusto Perez, Natalia Perkova, Guy Perrier, Slav Petrov, Daria Petrova, Jason Phelan, Jussi Piitulainen, Tommi A Pirinen, Emily Pitler, Barbara Plank, Thierry Poibeau, Larisa Ponomareva, Martin Popel, Lauma Pretkalniņa, Sophie Prévost, Prokopis Prokopidis, Adam Przepiórkowski, Tiina Puolakainen, Sampo Pyysalo, Peng Qi, Andriela Rääbis, Alexandre Rademaker, Taraka Rama, Loganathan Ramasamy, Carlos Ramisch, Fam Rashel, Mohammad Sadegh Rasooli, Vinit Ravishankar, Livy Real, Petru Rebeja, Siva Reddy, Georg Rehm, Ivan Riabov, Michael Riebler, Erika Rimkutė, Larissa Rinaldi, Laura Rituma, Luisa Rocha, Eiríkur Rögnvaldsson, Mykhailo Romanenko, Rudolf Rosa, Valentin Roşca, Davide Rovati, Olga Rudina, Jack Rueter, Kristján Rúnarsson, Shoval Sadde, Pegah Safari, Benoît Sagot, Aleksı Sahala, Shadi Saleh, Alessio Salomoni, Tanja Samardžić, Stephanie Samson, Manuela Sanguinetti, Ezgi Sanıyar, Dage Särg, Baiba Saulīte, Yanin Sawanakunanon, Shefali Saxena, Kevin Scannell, Salvatore Scarlata, Nathan Schneider, Sebastian Schuster, Lane Schwartz, Djame Seddah, Wolfgang Seeker, Mojgan Seraji, Mo Shen, Atsuko Shimada, Hiroyuki Shirasu, Yana Shishkina, Muh Shohibussirri, Dmitry Sichinava, Janine Siewert, Einar Freyr Sigurðsson, Aline Silveira, Natalia Silveira, Maria Simi, Radu Simionescu, Katalin Simkó, Mária Šimková, Kiril Simov, Maria Skachedubova, Aaron Smith, Isabela Soares-Bastos, Carolyn Spadine, Rachele Sprugnoli, Steinþór Steingrímsson, Antonio Stella, Milan Straka, Emmett Strickland, Jana Strnadová, Alane Suhr, Yogi Lesmana Sulestio, Umut Sulubacak, Shingo Suzuki, Zsolt Szántó, Dima Taji, Yuta Takahashi, Fabio Tamburini, Mary Ann C. Tan, Takaaki Tanaka, Samson Tella, Isabelle Tellier, Marinella Testori, Guillaume Thomas, Lisi Torga, Marsida Toska, Trond Trosterud, Anna Trukhina, Reut Tsarfaty, Utku Türk, Francis Tyers, Sumire Uematsu, Roman Untilov, Zdeňka Urešová, Larraitz Uriá, Hans Uszkoreit, Andrius Utka, Sowmya Vajjala, Rob van der Goot, Martine Vanhove, Daniel van Niekerk, Gertjan van Noord, Viktor Varga, Eric Villemonte de la Clergerie, Veronika	1221 1222 1223 1224 1225 1226 1227 1228 1229 1230 1231 1232 1233 1234 1235 1236 1237 1238 1239 1240 1241 1242 1243 1244 1245 1246 1247 1248 1249 1250 1251 1252 1253 1254 1255 1256 1257 1258 1259 1260 1261 1262 1263 1264 1265 1266 1267 1268 1269 1270 1271 1272 1273 1274 1275 1276 1277 1278 1279 1280 1281 1282 1283
------	--	--	--

1284	Vincze, Natalia Vlasova, Aya Wakasa, Joel C. Wallenberg, Lars Wallin, Abigail Walsh, Jing Xian Wang, Jonathan North Washington, Maximilan Wendt, Paul Widmer, Seyi Williams, Mats Wirén, Christian Wittern, Tsegay Woldemariam, Tak-sum Wong, Alina Wróblewska, Mary Yako, Kayo Yamashita, Naoki Yamazaki, Chunxiao Yan, Koichi Yasuoka, Marat M. Yavrumyan, Arife Betül Yenice, Olcay Taner Yıldız, Zhuoran Yu, Zdeněk Žabokrtský, Shorouq Zahra, Amir Zeldes, Hanzhi Zhu, Anna Zhuravleva, and Rayan Ziane. 2021. Universal dependencies 2.8 . LINDAT/CLARIAH-CZ digital library at the Institute of Formal and Applied Linguistics (ÚFAL), Faculty of Mathematics and Physics, Charles University.	
1298	Wei Zhang, Ziming Huang, Yada Zhu, Guangnan Ye, Xiaodong Cui, and Fan Zhang. 2021. On sample based explanation methods for NLP: Faithfulness, efficiency and semantic evaluation . In <i>Proceedings of the 59th Annual Meeting of the Association for Computational Linguistics and the 11th International Joint Conference on Natural Language Processing (Volume 1: Long Papers)</i> , pages 5399–5411, Online. Association for Computational Linguistics.	
1307	Vitalii Zhelezniak, Aleksandar Savkov, April Shen, and Nils Hammerla. 2019. Correlation coefficients and semantic textual similarity . In <i>Proceedings of the 2019 Conference of the North American Chapter of the Association for Computational Linguistics: Human Language Technologies, Volume 1 (Long and Short Papers)</i> , pages 951–962, Minneapolis, Minnesota. Association for Computational Linguistics.	
1315	Tianyuan Zhou, João Sedoc, and Jordan Rodu. 2019. Getting in shape: Word embedding subspaces . In <i>Proceedings of the 28th International Joint Conference on Artificial Intelligence (IJCAI)</i> , pages 5478–5484, Macao, China. ijcai.org.	
1320	Wenxuan Zhou, Bill Yuchen Lin, and Xiang Ren. 2021. Isobn: Fine-tuning BERT with isotropic batch normalization . In <i>Proceedings of the 35th AAAI Conference on Artificial Intelligence</i> , pages 14621–14629, Online. AAAI Press.	
	A Reproducibility	1325
	Our code and trained models are openly available at [URL] .	1326
		1327
	Implementation Our implementation is written in PyTorch version 1.10.0 (Paszke et al., 2019) for Python 3.9.5 and builds on code from the following repositories:	1328
		1329
		1330
		1331
	• https://github.com/huggingface/transformers version 4.9.2 (Wolf et al., 2020) for downloading, training, and evaluating models	1332
		1333
		1334
	• https://github.com/lxuechen/private-transformers version 0.1.0 (Li et al., 2021) for DP-training	1335
		1336
		1337
	• https://github.com/pdufter/minimult (Duffer and Schütze, 2020) for computing sentence retrieval precision	1338
		1339
		1340
	• https://github.com/jayroxis/CKA-similarity for computing CKA scores	1341
		1342
	• https://github.com/mlepori1/Picking_BERTs_Brain (Lepori and McCoy, 2020) for computing RSA scores	1343
		1344
		1345
	• https://github.com/bcbi-edu/p_eickhoff_isoscore (Rudman et al., 2021) for computing IsoScores	1346
		1347
		1348
	• https://github.com/FengNiMa/VAE-TracIn-pytorch (Kong and Chaudhuri, 2021) for computing TracInCP influence scores.	1349
		1350
		1351
	Model We use the pretrained XLM-RoBERTa (Conneau et al., 2020a) base model and tokenizer from https://huggingface.co/xlm-roberta-base .	1352
		1353
		1354
	Data We provide download links and references for the various datasets we used in Table 2.	1355
		1356
	Hardware We train on single Nvidia Titan RTX, A100 (both with CUDA version 11.0), and RTX 3090 (with CUDA version 11.5) GPUs. All machines have at least 64GB of RAM, which is required to compute the IsoScore for our larger evaluation sets (e.g., TED 2020 for POS).	1357
		1358
		1359
		1360
		1361
		1362
	Runtime Fine-tuning with evaluation during training on the Titan RTX, which is the slowest of the GPUs used, takes 2–3 hours for POS and 5–6 hours for XNLI. Computing TracInCP influence scores for one fine-tuned model takes about 30–45 minutes.	1363
		1364
		1365
		1366
		1367
		1368

Carbon Footprint Our fine-tuning runs accumulated ~ 36 compute days on the hardware mentioned above (most experiments were conducted on the less powerful Titan RTX GPUs) according to Weights & Biases²⁹, where we logged our experiments. Although we do not have precise numbers, a highly conservative estimate of the total compute spent including prototyping, hyperparameter search, and all our evaluations is ~ 75 compute days.

B (ϵ, δ) -Differential Privacy

In §2, we provide the definition of ϵ -differential privacy (DP), also called pure DP, as the basis for our theoretical exploration. In our experiments, we rely on (ϵ, δ) -DP (Dwork and Roth, 2014), also called approximate-DP, which is typically used in practice and relaxes the privacy guarantees by a (small) δ as follows:

A model \mathcal{M}_D induced from a dataset D is said to be (ϵ, δ) -differentially private iff for all datasets D, D' s.t. $D = D' \cup \{x_{diff}\}$, it holds that $\Pr[\mathcal{M}_D(x_{test}) = y] \leq \exp(\epsilon) \cdot \Pr[\mathcal{M}_{D'}(x_{test}) = y] + \delta$ for any x_{test} and y .

C Best Fine-Tuning Settings

As mentioned in §3, we pre-selected a set of suitable learning rates (LRs) for each task and ran 3 random initializations each. Based on the validation performance, we then selected the following 5 best settings for each privacy budget and task:

ϵ	POS LR (# Seeds)	XNLI LR (# Seeds)
1	$5e-4$ (2); $7e-4$ (3)	$3e-4$ (1); $4e-4$ (2); $5e-4$ (2)
3	$5e-4$ (2); $7e-4$ (3)	$3e-4$ (1); $4e-4$ (2); $5e-4$ (2)
8	$5e-4$ (3); $7e-4$ (2)	$4e-4$ (2); $5e-4$ (3)
15	$3e-4$ (1); $5e-4$ (2); $7e-4$ (2)	$3e-4$ (1); $4e-4$ (2); $5e-4$ (2)
30	$3e-4$ (1); $5e-4$ (2); $7e-4$ (2)	$3e-4$ (1); $4e-4$ (2); $5e-4$ (2)
∞	$5e-5$ (2); $7e-5$ (2); $1e-4$ (1)	$9e-5$ (2); $1e-4$ (3)

Table 4: Best 5 settings for each task and privacy budget. Includes LR and the corresponding number of random initializations (# seeds).

D IsoScore Algorithm

Algorithm 1 describes the IsoScore algorithm (Rudman et al., 2021).

E Further Analysis of RSA Results

As we see in §4, RSA aligns with sentence retrieval precision, CKA, and IsoScore in producing higher

²⁹<https://wandb.ai/>

scores for non-private models. However, there is a mismatch between RSA and the other metrics in highly private regimes, where our most private models ($\epsilon = 1$) do not exhibit high RSA scores. Instead, the aggregated RSA scores peak at medium levels of privacy ($\epsilon \in \{8, 15\}$) and for the non-private ($\epsilon = \infty$) models. Unlike for the other metrics, there is also no clear trend among our two tasks in terms of whether the pretrained or a randomly initialized XLM-R model scores higher in RSA.

A closer look at the non-aggregated results (Appendix Figures 9, 10, and 13) shows how the similarity patterns obtained from RSA are often unexpected. For instance, the similarities between the typologically distant languages FR and ZH are consistently high for the TED 2020 corpus whereas scores for typologically closer languages are lower (Fig. 9). Based on prior work by, for example, Pires et al. (2019), Wu and Dredze (2019), and Lauscher et al. (2020), we would expect the model to first compress similar languages before achieving compression for distant ones. Sometimes, we also observe extreme jumps in similarity between layers 0 and 8, for instance, between IT and TR in the Tatoeba corpus (Fig. 10). We do not find these jumps in CKA and sentence retrieval.

One reason why RSA scores may be more sensitive to stricter privacy guarantees (e.g., $\epsilon = 1$) is that the correlation between sentence vector distances is very sensitive to outliers. Differential privacy reduces the number of such outliers, effectively regularizing the correlation coefficients.

F Detailed Results for Experiments in §4

Figure 4 shows the development of the mean sentence retrieval precision at layer 8 for POS and XNLI over the course of fine-tuning with different privacy budgets.

We further present non-aggregated results for

- POS performance in Table 5
- XNLI performance in Table 6
- Sentence retrieval for POS in Figures 5 and 6
- Sentence retrieval for XNLI in Figure 11
- CKA for POS in Figures 7 and 8
- CKA for XNLI in Figure 12
- IsoScore for POS in Table 7
- IsoScore for XNLI in Table 8
- RSA for POS in Figures 9 and 10
- RSA for XNLI in Figure 13.

Algorithm 1 IsoScore (Rudman et al., 2021)

- 1: **begin** Let $X \subset \mathbb{R}^n$ be a finite collection of points.
 - 2: Let X^{PCA} denote the points in X transformed by the first n principal components.
 - 3: Define $\Sigma_D \in \mathbb{R}^n$ as the diagonal of the covariance matrix of X^{PCA} .
 - 4: Normalize diagonal to $\hat{\Sigma}_D := \sqrt{n} \cdot \Sigma_D / \|\Sigma_D\|$, where $\|\cdot\|$ is the standard Euclidean norm.
 - 5: The isotropy defect is $\delta(X) := \|\hat{\Sigma}_D - \mathbf{1}\| / \sqrt{2(n - \sqrt{n})}$, where $\mathbf{1} = (1, \dots, 1)^T \in \mathbb{R}^n$
 - 6: X uniformly occupies $\phi(X) := (n - \delta(X)^2(n - \sqrt{n}))^2 / n^2$ percent of ambient dimensions.
 - 7: Transform $\phi(X)$ so it can take values in $[0, 1]$, via $\iota(X) := (n \cdot \phi(X) - 1) / (n - 1)$.
 - 8: **return:** $\iota(X)$
 - 9: **end**
-

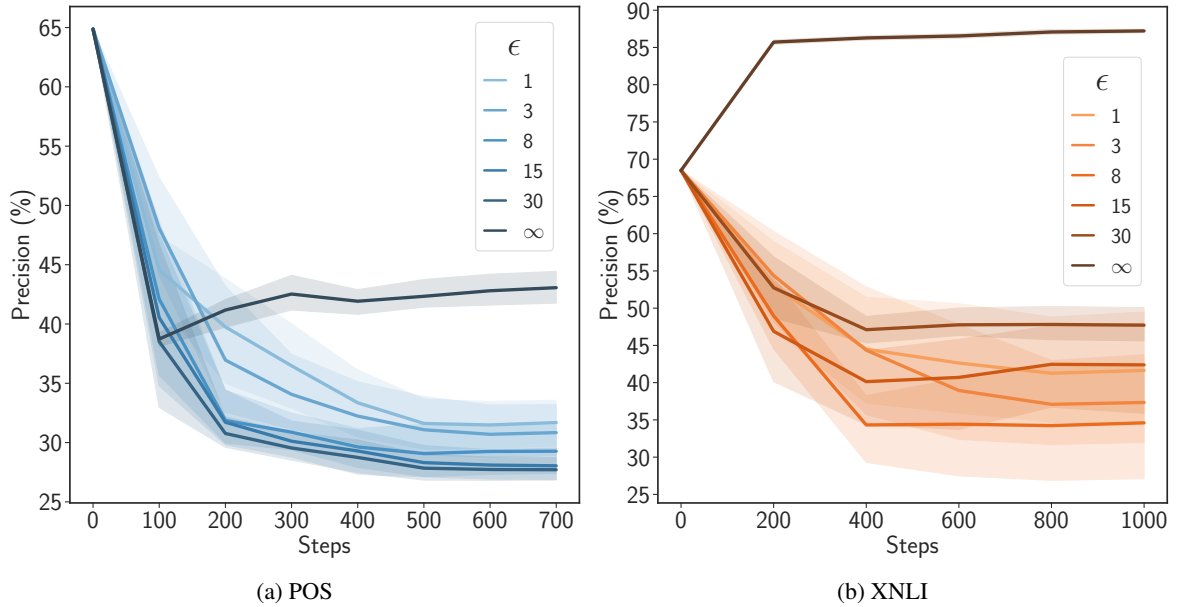


Figure 4: Mean sentence retrieval precision for our TED 2020 splits (different languages/data for POS and XNLI) at layer 8 over the course of fine-tuning with different privacy budgets (ϵ). $\epsilon = \infty$ denotes non-private models. Error bands show variation around the mean over 5 random seeds. At Steps = 0, all models are equivalent to the pretrained XLM-R Base. We see that the non-private models can retain (and for XNLI even improve) their multilingual compression much better than the private models and have less variation.

Dataset	Download Link	Reference
UD v2.8 (POS)	https://lindat.mff.cuni.cz/repository/xmlui/handle/11234/1-3683	(Nivre et al., 2020; Zeman et al., 2021)
XNLI	https://huggingface.co/datasets/xnli	(Conneau et al., 2018; Lhoest et al., 2021)
TED 2020	https://github.com/UKPLab/sentence-transformers/blob/master/docs/datasets/TED2020.md	(Reimers and Gurevych, 2020)
WikiMatrix	https://github.com/facebookresearch/LASER/tree/main/tasks/WikiMatrix	(Schwenk et al., 2021)
Tatoeba	https://github.com/LBeaudoux/tatoebatools	

Table 2: Links and references to the datasets we used in our experiments. License information are also available via these links. We ensure that we comply with respective license conditions and only use the data within their intended use policy where applicable.

Language	Treebank	# Sentences
AR	Arabic-PADT	680
DE	German-GSD	977
ES	Spanish-GSD	426
HI	Hindi-HDTB	1684
ID	Indonesian-GSD	557
KO	Korean-Kaist	2287
RU	Russian-SynTagRus	6491

Table 3: Overview of the UD v2.8 (Nivre et al., 2020; Zeman et al., 2021) treebanks (test splits only) that we use as test sets in our POS tagging experiments (§3.4) including their respective sizes (number of sentences).

ϵ	AR	DE	ES	HI	ID	KO	RU	AVG
1	68.3 / 64.6	75.5 / 75.1	79.8 / 79.0	65.0 / 63.3	73.8 / 71.9	66.1 / 54.2	74.8 / 74.0	71.9 / 68.9
3	79.1 / 76.6	86.6 / 86.8	90.3 / 89.3	74.4 / 70.9	82.6 / 79.4	71.1 / 59.4	86.1 / 86.3	81.4 / 78.4
8	81.0 / 77.6	88.4 / 88.3	91.6 / 90.2	78.2 / 75.6	84.2 / 81.2	70.8 / 60.9	87.1 / 87.4	83.0 / 80.2
15	81.3 / 78.4	88.8 / 89.0	92.4 / 90.9	77.0 / 73.2	83.9 / 80.7	71.9 / 61.8	87.7 / 87.8	83.3 / 80.3
30	81.8 / 78.7	89.4 / 89.6	92.9 / 91.5	77.6 / 74.0	84.3 / 81.1	72.3 / 62.2	88.2 / 88.4	83.8 / 80.8
∞	83.8 / 79.7	91.5 / 91.2	95.0 / 93.2	82.8 / 80.2	86.2 / 81.3	74.2 / 62.9	89.9 / 90.2	86.2 / 82.7

Table 5: **POS** Performance (validation / test accuracy) when fine-tuning XLM-R Base with different privacy budgets (ϵ). We show results averaged over 5 random seeds each. $\epsilon = \infty$ denotes non-private models. AVG is the average over the 7 languages. See §3 for our experimental setup. We see that performance increases with decreased privacy across all languages.

ϵ	AR	DE	EL	RU	SW	TH	UR	AVG
1	37.3 / 37.4	36.8 / 37.0	36.6 / 36.5	36.3 / 36.2	34.3 / 34.5	35.6 / 35.7	35.6 / 35.6	36.1 / 36.1
3	49.6 / 50.3	49.3 / 51.0	50.8 / 51.5	49.7 / 50.2	45.9 / 47.2	48.8 / 49.5	47.6 / 48.2	48.8 / 49.7
8	55.9 / 56.4	56.8 / 58.5	58.2 / 58.1	56.3 / 57.1	52.0 / 53.2	55.6 / 55.7	53.3 / 53.7	55.5 / 56.1
15	59.1 / 58.3	60.4 / 60.8	61.5 / 60.9	59.7 / 59.5	54.4 / 54.8	58.9 / 58.2	56.4 / 56.1	58.6 / 58.4
30	61.6 / 60.8	63.6 / 63.1	64.8 / 62.0	62.0 / 61.1	56.5 / 57.3	61.2 / 60.2	58.6 / 57.8	61.2 / 60.3
∞	90.9 / 67.8	96.2 / 70.5	95.5 / 70.1	93.4 / 69.7	79.0 / 62.5	91.6 / 68.5	86.8 / 65.4	90.5 / 67.8

Table 6: **XNLI** Performance (validation / test accuracy) when fine-tuning XLM-R Base with different privacy budgets (ϵ). We show results averaged over 5 random seeds each. $\epsilon = \infty$ denotes non-private models. AVG is the average over the 7 languages. See §3 for our experimental setup. We see that performance increases with decreased privacy across all languages. Here, we also particularly observe that the gap between validation and test performance is substantially lower for private models, which shows the strong regularization effect of training with differential privacy.

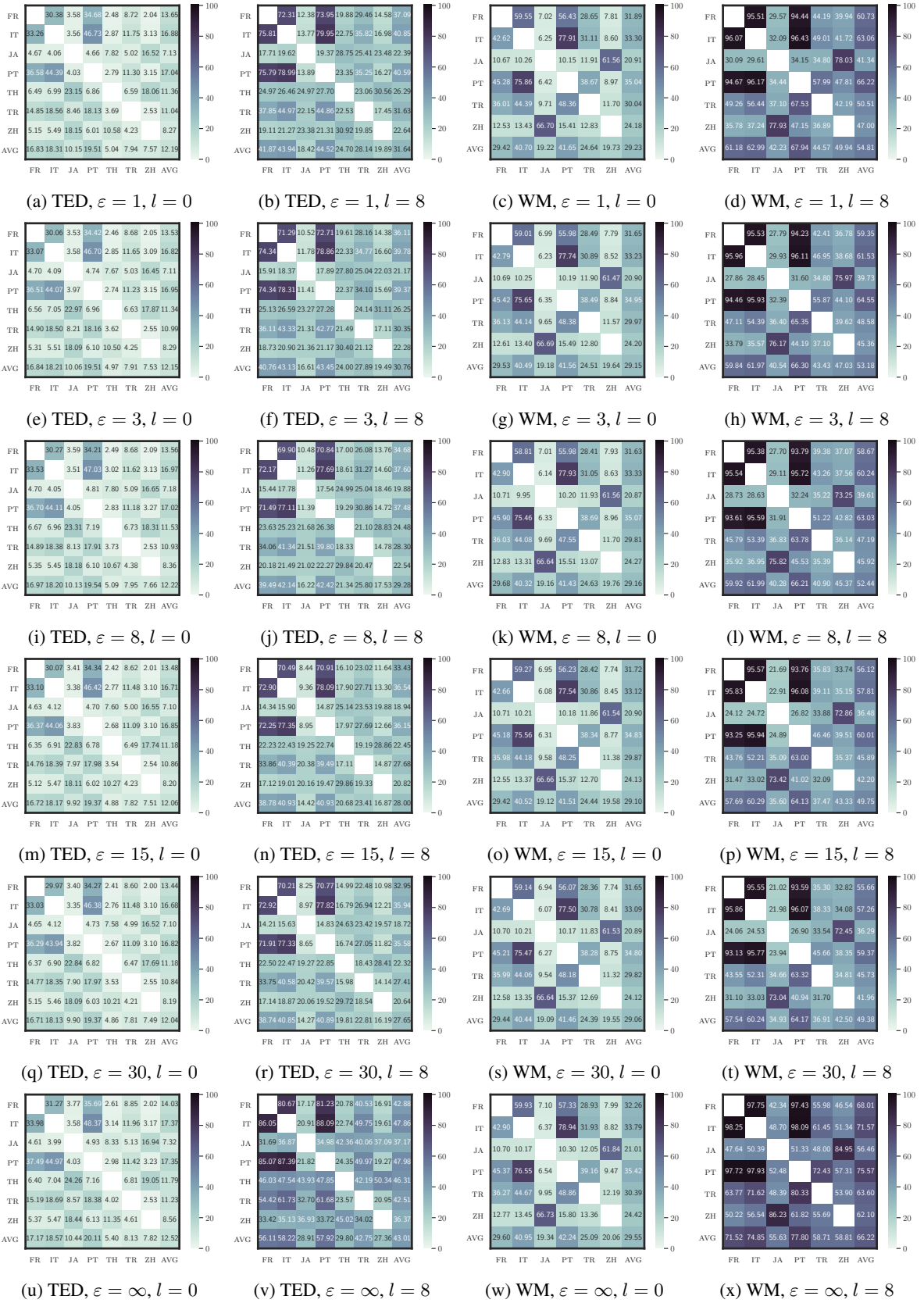


Figure 5: POS Sentence retrieval results for the TED 2020 (TED) and WikiMatrix (WM) datasets and different combinations of privacy budgets (ε) and layers (l). Each heatmap cell corresponds to the average over 5 random seeds. We observe that the overall patterns are highly similar across all levels of privacy and particularly at layer 0.

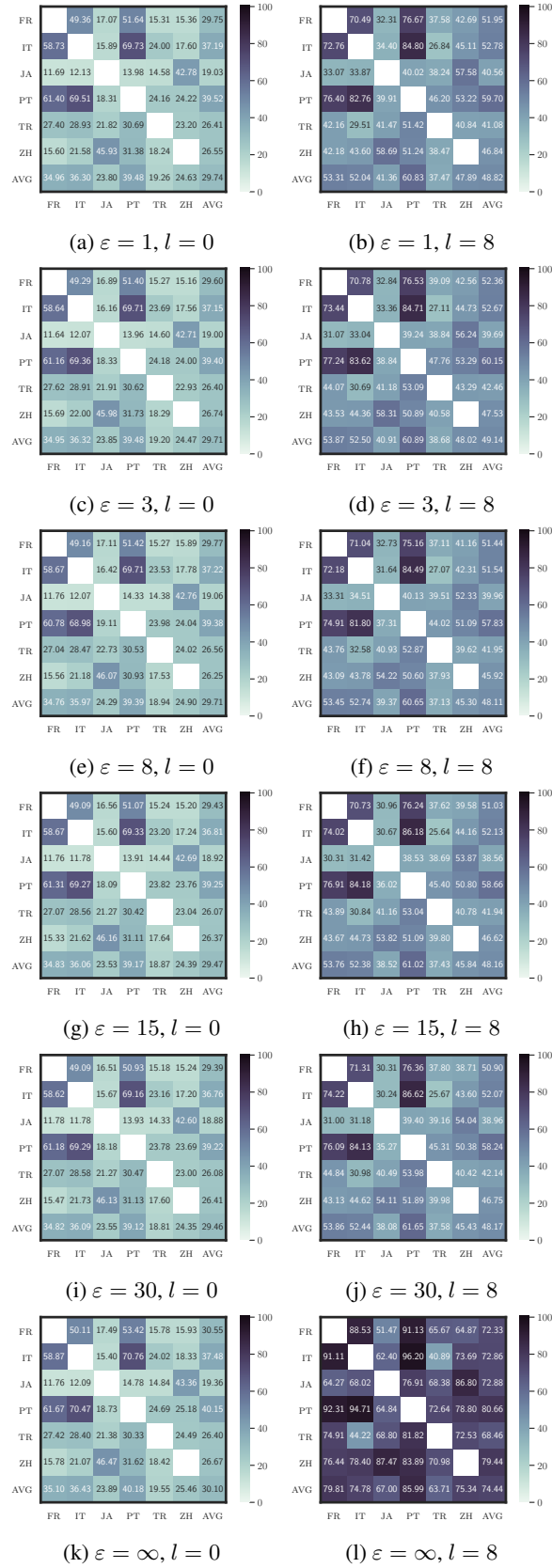


Figure 6: **POS** sentence retrieval results for the Tatoeba dataset and different combinations of privacy budgets (ε) and layers (l). Each heatmap cell corresponds to the average over 5 random seeds. We observe that the overall patterns are highly similar across all levels of privacy and particularly at layer 0.

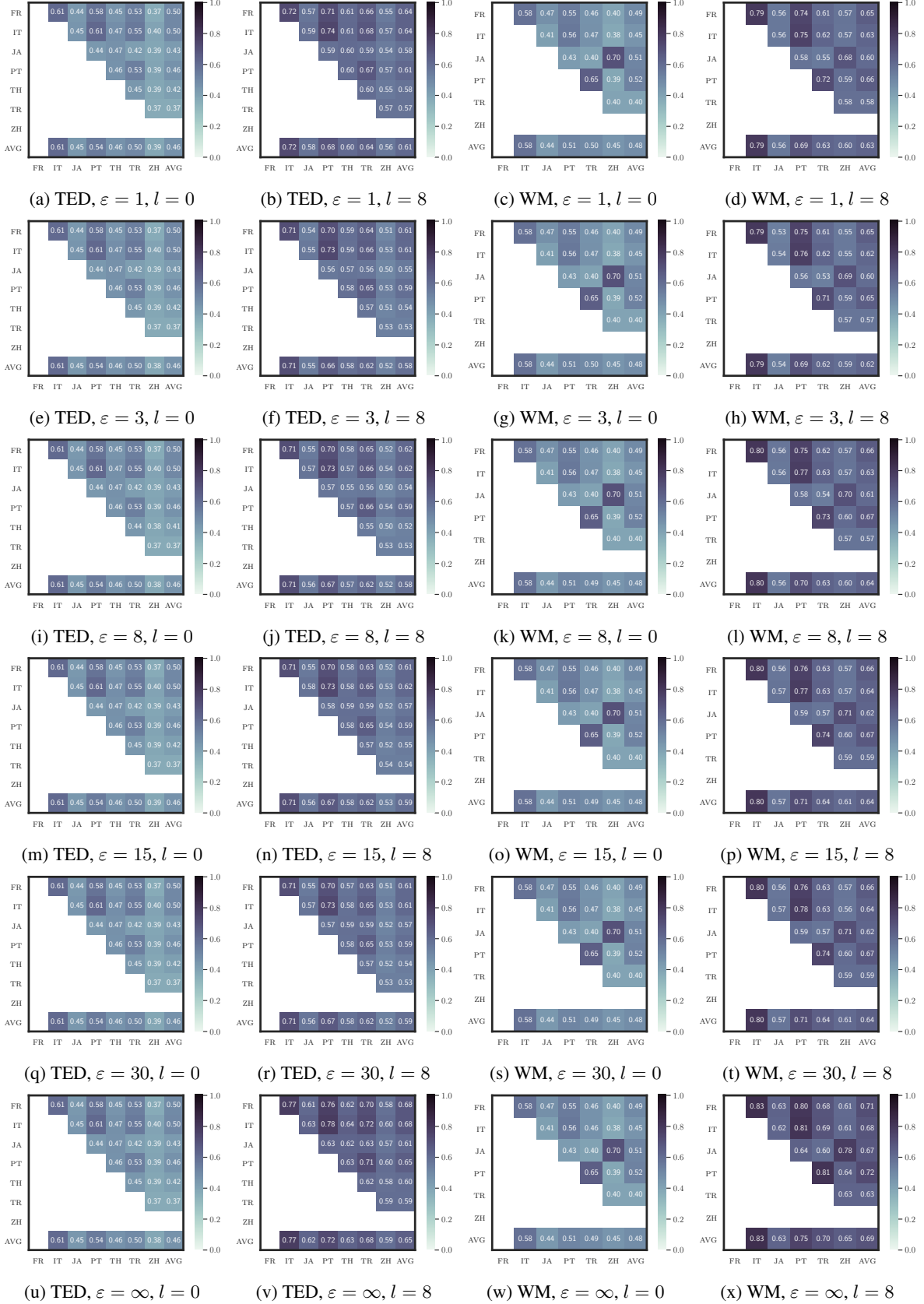


Figure 7: POS CKA results for the TED 2020 (TED) and WikiMatrix (WM) datasets and different combinations of privacy budgets (ε) and layers (l). Each heatmap cell corresponds to the average over 5 random seeds. We observe that the overall patterns are highly similar across all levels of privacy and particularly at layer 0.

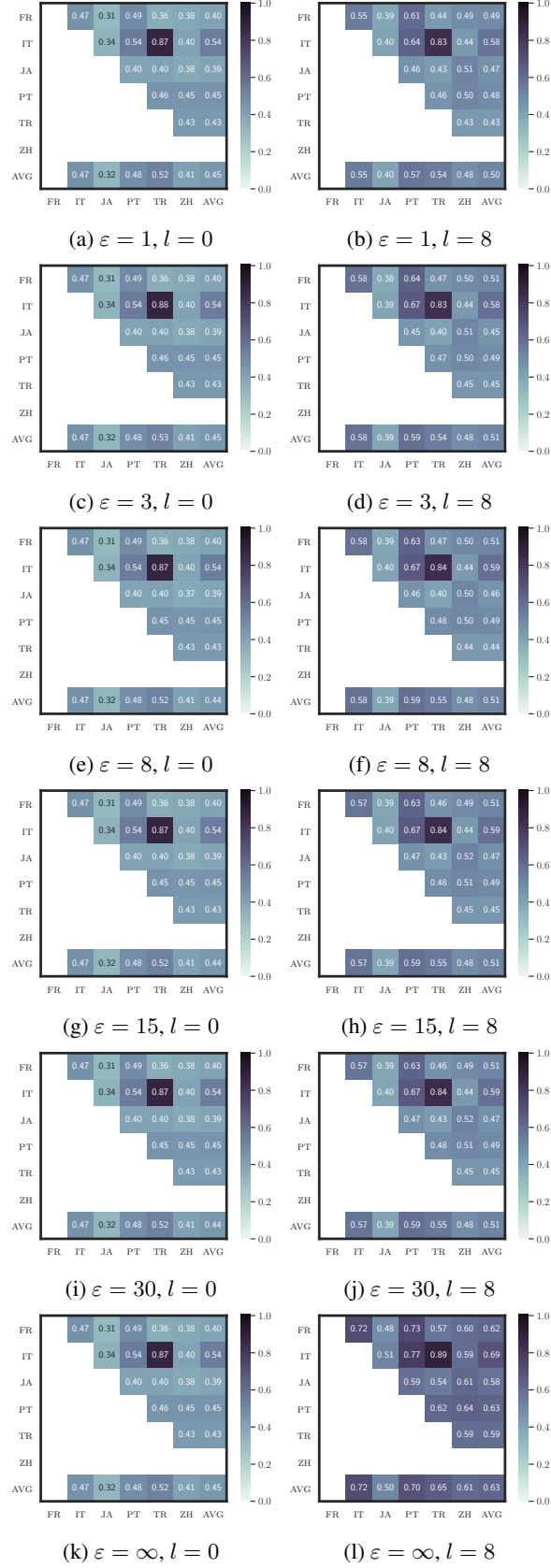


Figure 8: POS CKA results for the Tatoeba dataset and different combinations of privacy budgets (ϵ) and layers (l). Each heatmap cell corresponds to the average over 5 random seeds. We observe that the overall patterns are highly similar across all levels of privacy and particularly at layer 0.

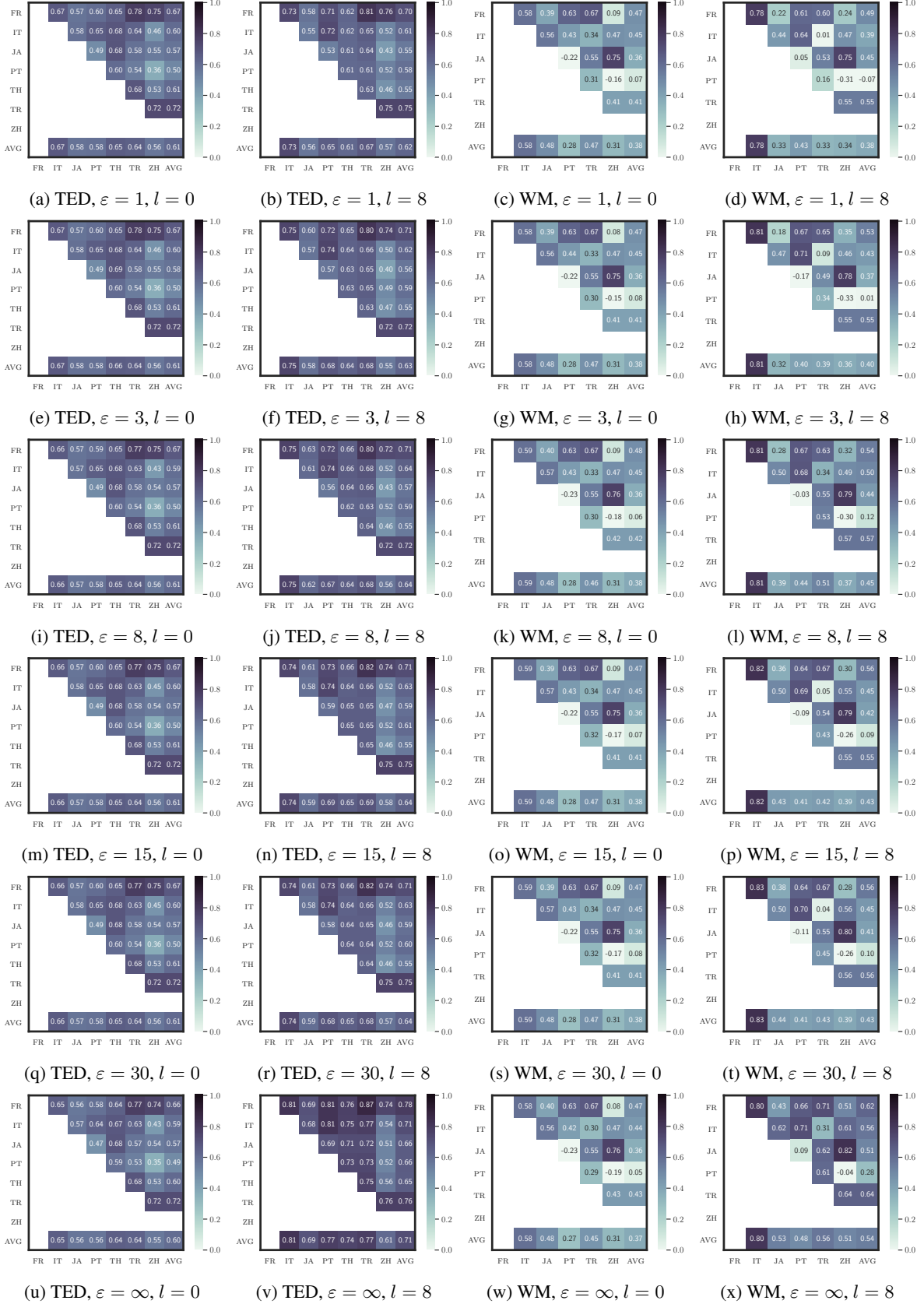


Figure 9: POS RSA results for the TED 2020 (TED) and WikiMatrix (WM) datasets and different combinations of privacy budgets (ϵ) and layers (l). Each heatmap cell corresponds to the average over 5 random seeds. We observe that the overall patterns are highly similar across all levels of privacy and particularly at layer 0.

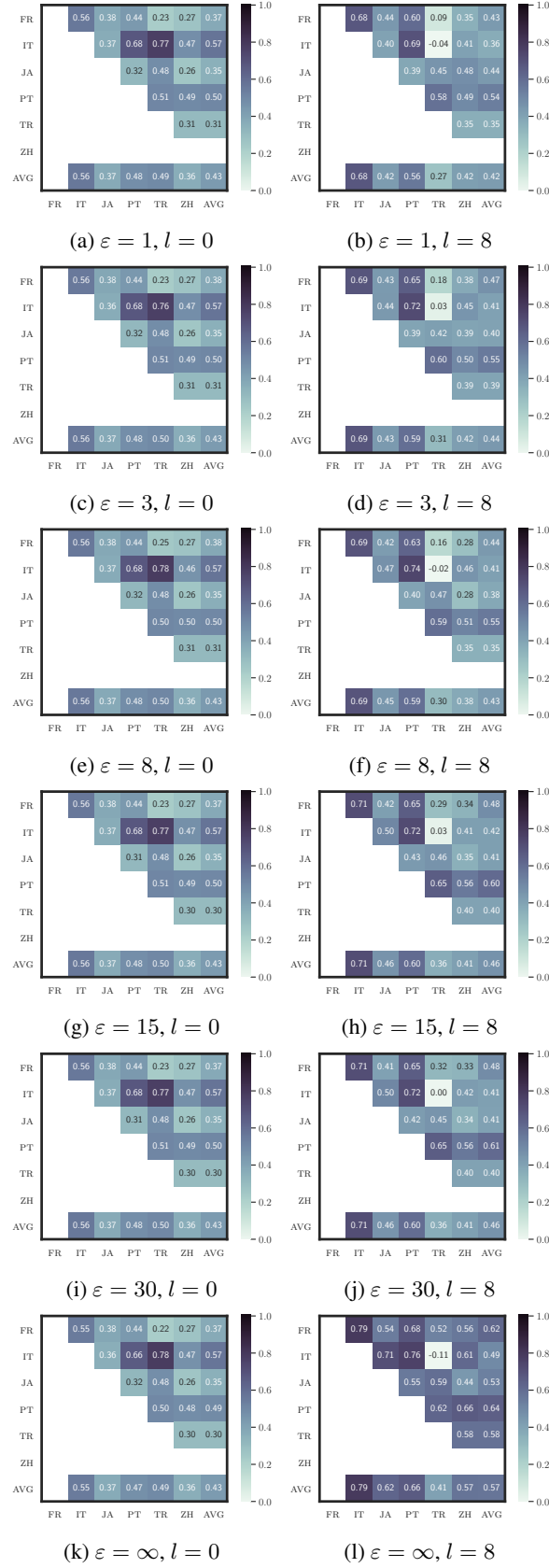


Figure 10: POS RSA results for the Tatoeba dataset and different combinations of privacy budgets (ε) and layers (l). Each heatmap cell corresponds to the average over 5 random seeds. We observe that the overall patterns are highly similar across all levels of privacy and particularly at layer 0. Also note that, unlike in CKA (Figure 8), the similarity between IT and TR is high at layer 0 but low at layer 8.

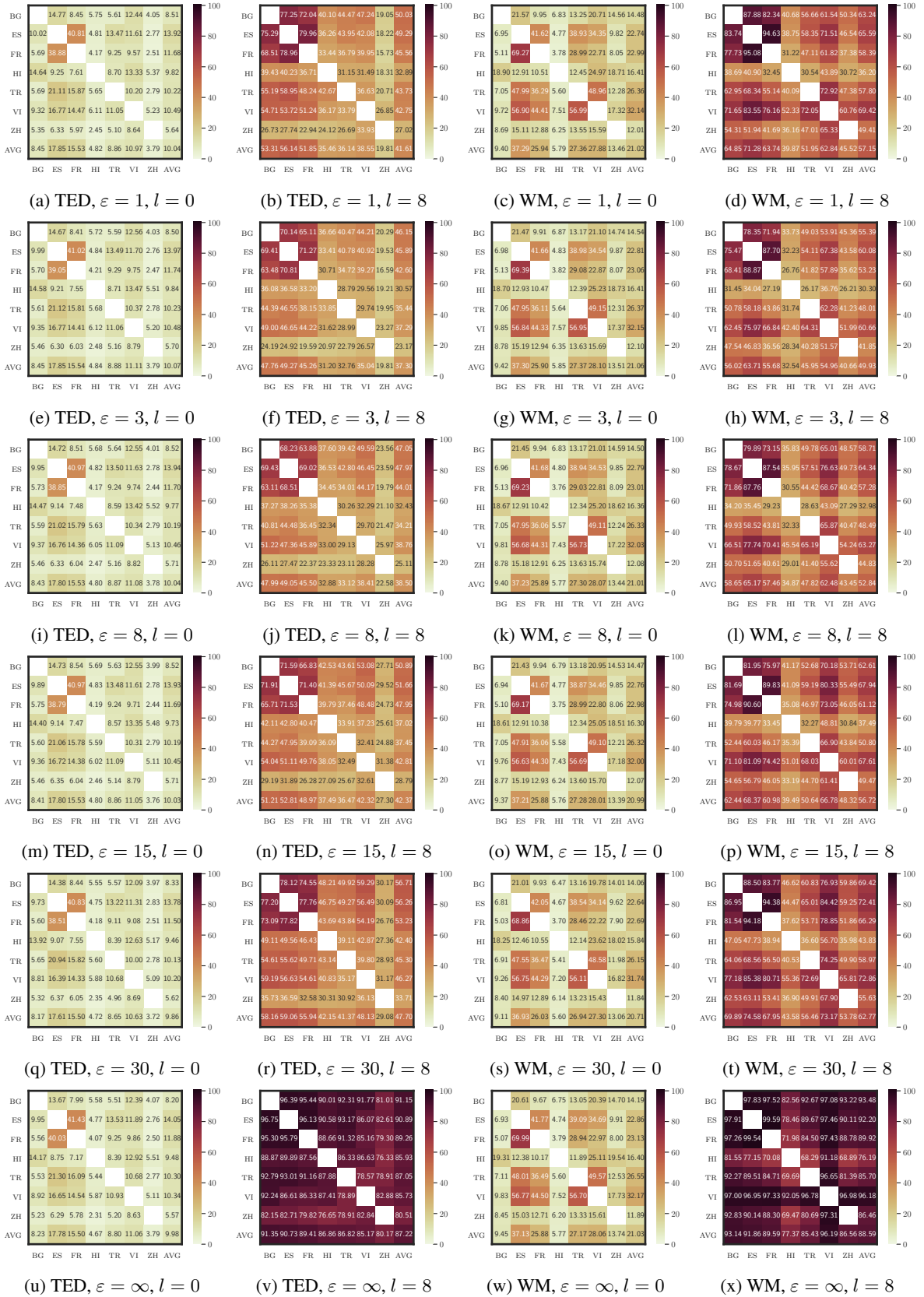


Figure 11: XNLI Sentence retrieval results for the TED 2020 (TED) and WikiMatrix (WM) datasets and different combinations of privacy budgets (ε) and layers (l). Each heatmap cell corresponds to the average over 5 random seeds. We observe that the overall patterns are highly similar across all levels of privacy and particularly at layer 0.

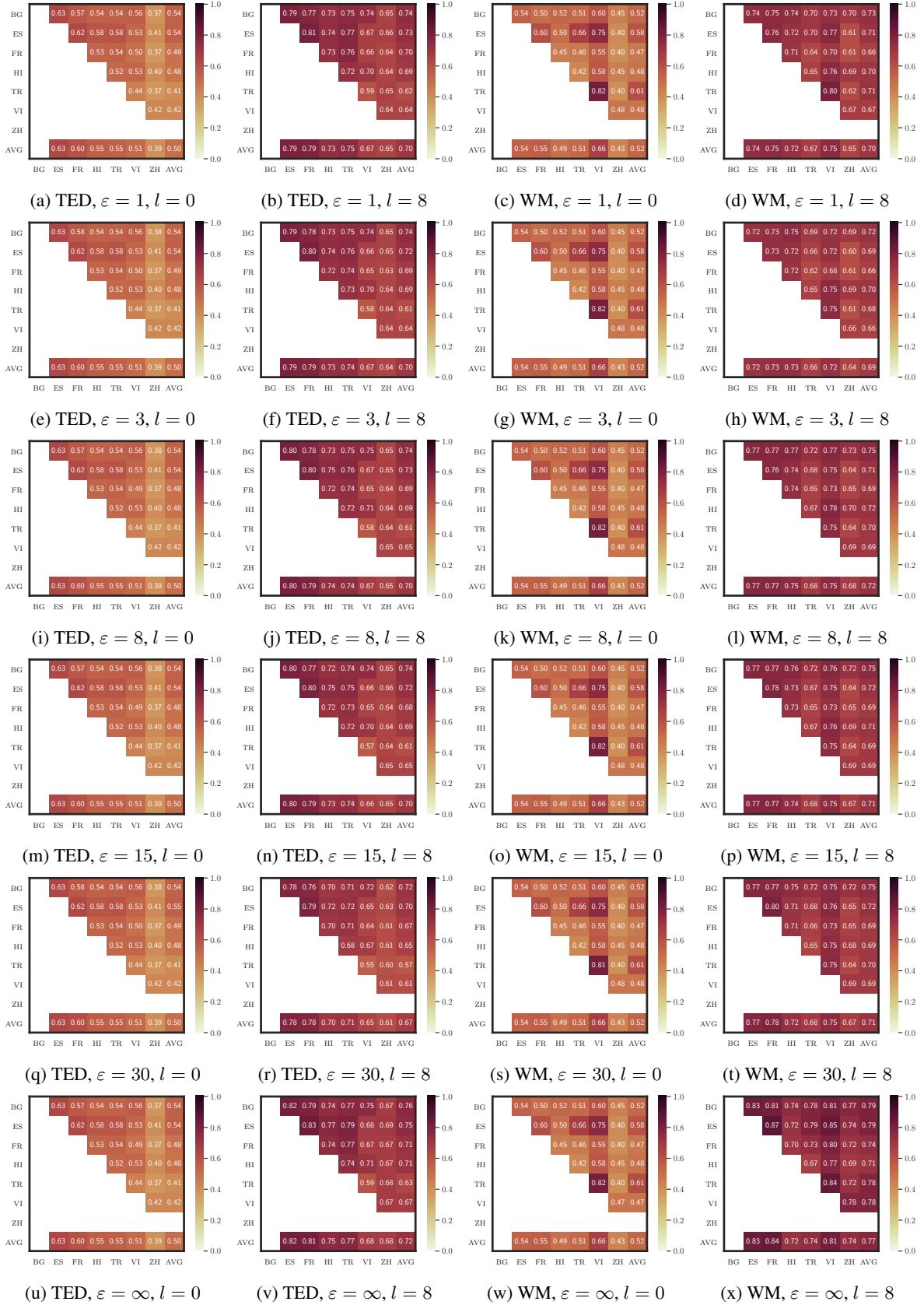


Figure 12: XNLI CKA results for the TED 2020 (TED) and WikiMatrix (WM) datasets and different combinations of privacy budgets (ε) and layers (l). Each heatmap cell corresponds to the average over 5 random seeds. We observe that the overall patterns are highly similar across all levels of privacy and particularly at layer 0.

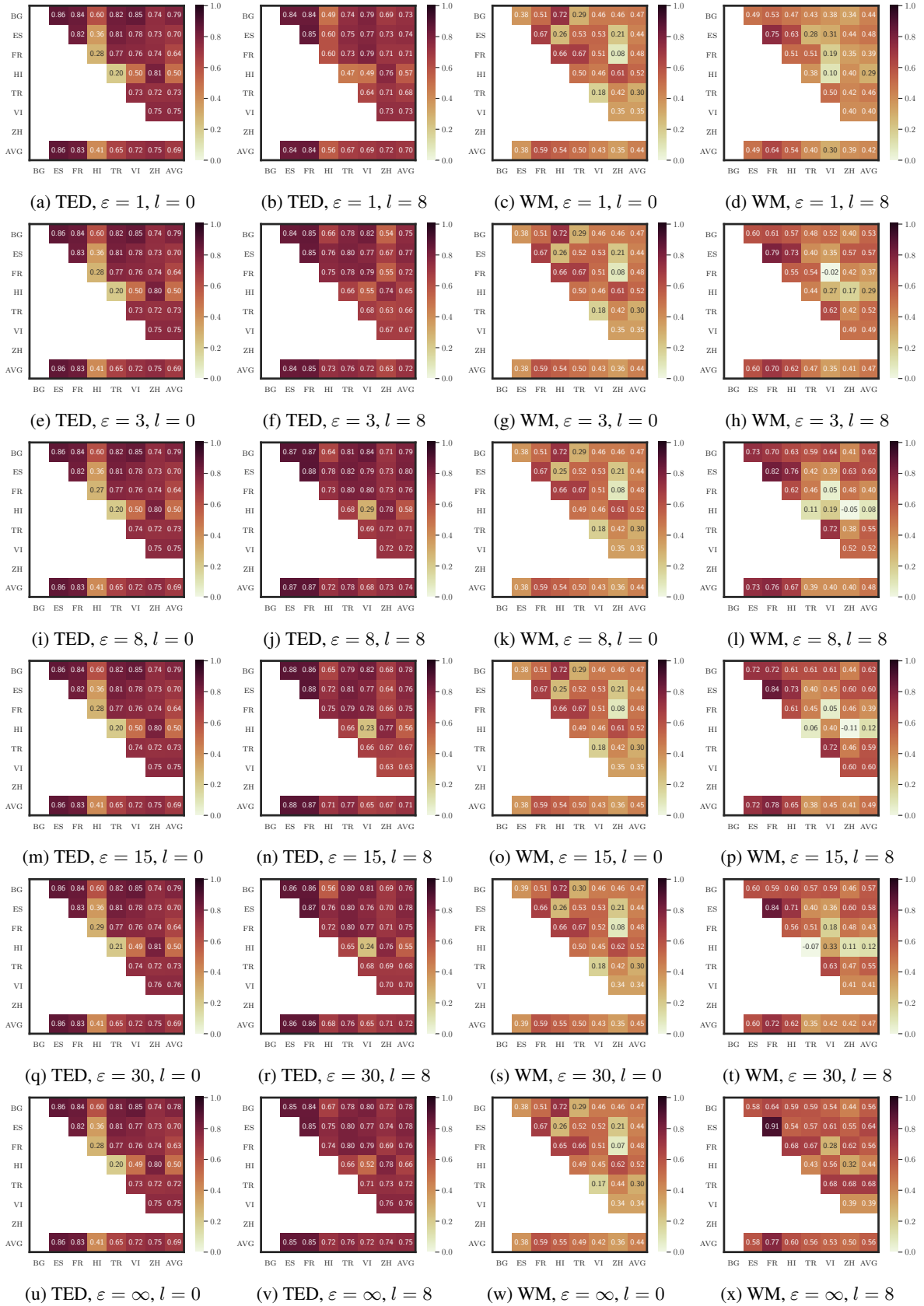


Figure 13: XNLI RSA results for the TED 2020 (TED) and WikiMatrix (WM) datasets and different combinations of privacy budgets (ε) and layers (l). Each heatmap cell corresponds to the average over 5 random seeds. We observe that the overall patterns are highly similar across all levels of privacy and particularly at layer 0.

ϵ	TED 2020		WikiMatrix		Tatoeba	
	$l = 0$	$l = 8$	$l = 0$	$l = 8$	$l = 0$	$l = 8$
RND	0.141	0.132	0.114	0.111	0.054	0.061
PRE	0.187	0.130	0.198	0.112	0.134	0.075
1	0.188	0.054	0.199	0.046	0.135	0.033
3	0.188	0.044	0.199	0.038	0.135	0.027
8	0.187	0.045	0.197	0.038	0.133	0.027
15	0.187	0.047	0.199	0.040	0.135	0.028
30	0.187	0.047	0.199	0.040	0.135	0.028
∞	0.188	0.087	0.199	0.070	0.135	0.051

Table 7: **POS** IsoScores for different combinations of privacy budgets (ϵ) and layers (l). We show results averaged over 5 random seeds, except for RND and PRE. RND and PRE (added for comparison) denote XLM-R with randomly initialized weights and the original pretrained XLM-R, respectively. We see that the isotropy is fairly uniform across privacy budgets at layer 0 and generally higher at layer 0 than at layer 8. At layer 8, it peaks for non-private ($\epsilon = \infty$) and our most private ($\epsilon = 1$) models.

ϵ	TED 2020		WikiMatrix	
	$l = 0$	$l = 8$	$l = 0$	$l = 8$
RND	0.144	0.134	0.130	0.124
PRE	0.195	0.138	0.210	0.129
1	0.195	0.121	0.211	0.120
3	0.196	0.101	0.211	0.104
8	0.196	0.074	0.212	0.079
15	0.196	0.071	0.212	0.077
30	0.194	0.087	0.210	0.089
∞	0.195	0.182	0.211	0.166

Table 8: **XNLI** IsoScores for different combinations of privacy budgets (ϵ) and layers (l). We show results averaged over 5 random seeds, except for RND and PRE. RND and PRE (added for comparison) denote XLM-R with randomly initialized weights and the original pretrained XLM-R, respectively. We see that the isotropy is fairly uniform across privacy budgets at layer 0 and generally higher at layer 0 than at layer 8. At layer 8, it peaks for non-private ($\epsilon = \infty$) and our most private ($\epsilon = 1$) models.